Oxygen Abundances in Two Metal-poor Subgiants from the Analysis of the λ 6300 Å Forbidden O I Line

UCO/Lick Observatory,	Jon P. Fulbright ¹ Dept of Astronomy,	and Robert University	of California,	Santa	Cruz,	CA	95064
Received	;	accepte	d				

 1 Email: jfulb@ucolick.org

 $^2\mathrm{Email:}\ \mathrm{kraft@ucolick.org}$

ABSTRACT

Recent LTE analyses (Israelian et al. 1998, Boesgaard et al 1999) of the OH bands in the optical ultraviolet spectra of nearby metal-poor subdwarfs indicate that oxygen abundances are generally higher than those previously determined from the analysis of the [O I] doublet in the spectra of low-metallicity giants. On average, the difference increases with decreasing metallicity and reaches $\Delta [O/Fe] \sim +0.6$ dex as [Fe/H] approaches -3.0. Employing high resolution (R = 50000), high S/N (~ 250) echelle spectra of the two stars found by Israelian et al. (1998) to have the highest [O/Fe]-ratios, viz, BD +23 3130 and BD +37 1458, we conducted abundance analyses based on about 60 Fe I and 7-9 Fe II lines. We determined from Kurucz LTE models the appropriate values of T_{eff} , log g, [Fe/H], v_t , as well as abundances of Na, Ni, and the traditional alpha-elements Mg, Si, Ca and Ti, independent of the calibration of color vs T_{eff} scales. We determined oxygen abundances from spectral synthesis of the stronger line (λ 6300 Å) of the [O I] doublet. The ionization equilibrium of Fe indicates that these two stars are subgiants, rather than subdwarfs, and our derived values of T_{eff} are 150 to 300K lower than those assumed by the previous investigators, although the resulting [Fe/H]-values differ only slightly. The syntheses of the [O I] line lead to smaller values of [O/Fe], consistent with those found earlier among halo field and globular cluster giants. We obtain $[O/Fe] = +0.35 \pm 0.2$ for BD +23 3130 and +0.50 ± 0.2 for BD +37 1458. In the former, the [O I] line is very weak (~ 1 mÅ), so that the quoted [O/Fe] value may in reality be an upper limit. Therefore in these two stars a discrepancy exists between the [O/Fe]- ratios derived from [O I] and the OH feature, and the origin of this difference remains unclear. Until the matter is clarified, we suggest it is premature to conclude that the ab initio oxygen abundances of old, metal-poor stars need to be revised drastically upward.

1. Introduction

After hydrogen and helium, oxygen is the most abundant element in the Universe. It is well-known that knowledge of [O/Fe]-ratios in old, metal-poor stars is required if one is to test theories of Galactic chemical evolution. In addition, the oxygen abundance also affects both the energy generation and opacity of stars near the main sequence turnoff region of the color-magnitude diagram, and thus affects the determination of ages of globular clusters and the oldest stars (Rood & Crocker 1985, VandenBerg 1985). The sensitivity of age to [O/Fe] is not negligible: according to VandenBerg (1992), the gradient is $\Delta T/\Delta$ [O/Fe] = -4 Gyr/ 1 dex. Until recently, most determinations of [O/Fe] among old, metal-poor stars, have been confined to the analysis of the forbidden [O I] doublet at $\lambda\lambda$ 6300, 6364 Å. These transitions arise from the ground state and appear in absorption in the sun and also in metal-poor giants. All such studies agree (cf. reviews by Suntzeff 1993, Kraft 1994, Briley et al. 1994, McWilliam 1997) that [O/Fe] increases from ~ 0.0 at solar metallicity to a value near +0.4 at $[Fe/H] \sim -1.0$, after which [O/Fe] levels off near this last-named value and is essentially constant (with some scatter) to metal-poor values as low as $[Fe/H] \sim -3$. The behavior of oxygen therefore mimics that of the other so-called alpha elements, e.g., Mg, Si and Ca. The only exception seems to be the behavior of [O/Fe] among globular

cluster giants where, presumably as a result of deep mixing of the stellar envelope through the CNO hydrogen-burning shell, oxygen is significantly depleted, sometimes well below the value $[O/Fe] \sim 0.0$, and transmuted to nitrogen (e.g., Kraft et al. 1997).

Apparently oxygen depletion among field halo giants, similar to that experienced by globular cluster giants, does not take place (Hanson et al. 1998). However, since main sequence stars do not mix their surface layers into regions where oxygen depletion could occur, one naturally assumes that oxygen abundances determined from subdwarfs would be more secure than those determined from their giant star analogues. Unfortunately, it is impractical to use the [O I] doublet to determine [O/Fe] among metal-poor subdwarfs. Owing to that fact that these stars are generally hotter, have higher atmospheric density and have much decreased ratio of line to continuous opacity in comparison with giants, the $\lambda\lambda$ 6300, 6364 Å lines virtually disappear from their spectra. The solar EW of λ 6300 Å, the stronger of the two forbidden lines, is 6 mÅ. In a giant of metallicity [Fe/H] = -2.2, for example, the EW(6300) ~ 30 mÅ when [O/Fe] = +0.4 (e.g., Sneden et al. 1997). We calculated model synthetic spectra of the λ 6300 Å region in a subdwarf having solar values of T_{eff} and log g and also having [Fe/H] = -2.2 and found that EW(6300) = 1 mÅ, even for an [O/Fe]-ratio as large as +1.0. High resolution, high S/N analysis of the two well-known subdwarfs HD 74000 and HD 25329 (Beveridge & Sneden 1994) confirms this surmise. Clearly the discrimination of [O/Fe]-values among very metal-poor subdwarfs in the [O/Fe]-range 0.0 to +1.0 is beyond present observational capabilities, if one employs only the forbidden [O I] doublet.

The IR permitted O I triplet lines centered near λ 7774 Å provide an alternative means of estimating [O/Fe], their EWs being in the 10-20 mÅ range even for very metal-poor subdwarfs having T_{eff} and log g similar to that of the sun (Abia & Rebolo 1989). Analysis of these lines has in general led to values of [O/Fe] several tenths dex higher than those derived from the [O I] lines in metal-poor giants (Abia & Rebolo 1989, Tomkin et al. 1992, Cavallo et al. 1997). The discrepancy increases with decreasing metallicity and amounts to more than 0.5 dex as [Fe/H] approaches -3. Since the triplet lines arise from a level more than 9 eV above the ground state of the oxygen atom, King (1993) suggested that an increase in the adopted T_{eff} scale (Carney 1983) of subdwarfs by 150-200K would resolve the problem. This solution was criticized by Balachandran & Carney (1996), who, in analyzing the infrared OH and CO bands of the well-known, intermediately metal-poor ([Fe/H] = -1.22) subdwarf HD 103095, determined the low oxygen abundance of [O/Fe] = +0.29, consistent with the originally adopted Carney (1983) T_{eff} scale. Other approaches to the problem involving radiative transfer (Kisselman & Nordlund 1995) and chromospheric heating (Takeda 1995) effects have also been invoked, but a generally agreed upon solution has not be forthcoming.

Analysis of the low-excitation bands of OH, which lie in the (optical) UV just longward of the atmospheric cutoff, provides a third means of obtaining [O/Fe]-ratios (Bessell et al. 1984), but the procedure is rendered difficult because of flux limitations and severe line blending even in metal-poor stars. Bessell et al. (1991) and Nissen et al. (1994) derived [O/Fe]-values for a few metal-poor stars, and concluded that these were in agreement with values derived from analysis of the [O I] lines. Recently, however, an analysis of 23 stars, mostly low-metallicity subdwarfs, based on the UV OH features, has led to the conclusion (Israelian et al. 1998, hereafter I98) that oxygen is strongly overabundant, the

[O/Fe]-ratio increasing from ~+0.6 to ~+1.0 as [Fe/H] decreased from -1.5 to -3.0. These results are in close agreement with the results obtained earlier from the IR permitted oxygen triplet. A similar conclusion has been reached from a study of 24 (mostly) unevolved low-metallicity stars (Boesgaard et al 1999, hereafter B99), again based on the UV OH bands. If these higher [O/Fe]-values are indeed correct, three conclusions emerge, if at the same time, the smaller [O/Fe]- values derived for giants from analysis of the [O I] lines are also correct. First, all metal-poor giants must indeed have undergone deep mixing which has permitted the ashes of O to N processing to reach the surface. This would, of necessity, be true for halo giants, even those not members of globular clusters. Moreover, even those globular cluster giants having [O/Fe] near +0.4 must themselves also have undergone deep mixing. Second, oxygen does not share the same degree of modest "overabundance" as do other alpha elements such as Mg, Si and Ca, all of which are predicted to arise from the same nucleosynthetic processes in Type II supernovae (e.g. Arnett 1995, Fig 1). Finally, the ages of globular clusters are presumably 1 to 2 Gyr younger than one would have inferred from the [O I]-based oxygen abundances (VandenBerg 1985, Chaboyer et al. 1998).

It is also possible, of course, that the disagreement between the oxygen abundances arises not because of some real physical effect, but rather from some inadequacy of the analysis or modelling procedure. We have already noted that, among low-metallicity subdwarfs, the [O I] lines become too weak to provide useful discriminatory input when [O/Fe] < +1.0. However, two stars in the list of I98, BD +23 3130 and BD +37 1458, are actually subgiants: their spectra, as we shall show, contain measureable lines of the [O I] doublet. These two stars are also the most overabundant in oxygen of all stars in the I98 list, with [O/Fe] values, derived from the UV OH bands, of +1.17 and +0.97, respectively. The star BD +37 1458 is also to be found in the list by B99, for which they derive a similarly large oxygen abundance of [O/Fe] = +0.83 (King 1993 T_{eff} scale).

The remainder of this paper concerns the analysis of [O/Fe] for these two subgiants, making use of observations of the λ 6300 [O~I] line derived from high resolution, high S/N spectra. We conduct a full LTE analysis of a large sample of Fe I and Fe II lines, from which we determine T_{eff} and log g directly from Kurucz model atmospheres, without appealing to temperature scales derived from colors. This procedure leads to oxygen abundances that do not agree with those derived either from the IR triplet permitted lines or the UV OH bands. Instead, we derive [O/Fe]-values that are consistent with those derived from analysis of [O~I]-doublet in bright, low-metallicity field giants.

2. Observations and Reductions

The two stars selected for observation, BD +23 3130 and BD +37 1458, were taken from the lists of metal-poor stars analyzed by I98 and B99 because we inferred that their surface gravities corresponded more closely to subgiants than subdwarfs. As such, we suspected that they would have measureable [O I] lines at λ 6300 Å. Both stars were observed on two different nights using the Hamilton Echelle Spectrograph (Vogt 1987), operated at the coude focus of the Shane 3-m Telescope of Lick Observatory. The spectrograph was set at a (two pixel) spectral resolution of R = 50,000. The CCD detector was a thinned, cosmetically excellent, LL2-LA6-0 chip with dimensions of 2048 x 2048 pixels. Observational

details are listed in Table 1.

The frames were reduced using standard IRAF routines. First the overscan pedestal was removed, followed by the bias. A normalized flat field was created from several quartz exposures, and used to correct the pixel-to- pixel variations. Occasional bad columns were corrected by interpolation. After apertures were defined and traced, the frames were corrected for scattered light and the spectra extracted. Finally, a wavelength solution, created from Th/A lamp exposures, was attached to the extracted spectra.

During both nights of observation, extremely high S/N spectra were taken of hot, rapidly rotating stars. These were used to remove the atmospheric O_2 lines present in the λ 6300 Å spectral region. Following the procedures outlined in detail elsewhere (e.g., Shetrone 1996), the hot star spectra were adjusted in strength so that the O_2 lines matched those of the program star; the adjusted hot star spectrum was then divided from the program star. Fortunately the [O I] line did not lie near an O_2 feature in either star, but the $\lambda\lambda$ 6297 Å and 6301 Å Fe I lines of BD +23 3130 were blended with atmospheric O_2 lines, as was the λ 6301 Å Fe I line of BD +37 1458. Thus great care was taken in matching the O_2 features of the hot star with those of the program objects. None of these Fe I lines were used to determine the atmospheric parameters of either program star. The corrected spectrum of this region is, however, shown in the syntheses discussed later (see Section 5), in which the flat fielding was accomplished using the hot stars themselves, without using the quartz exposures. Experience shows (e.g., Sneden et al. 1991) that hot-star flatfields are superior to quartz flatfields as a basis for testing synthetic spectra, especially of weak lines, possibly because the hot star beam fills the collimator of the spectrograph in the same manner as does the beam of the program star. Finally, we estimate that the resulting program star spectra have a S/N \sim 250 in the vicinity of the λ 6300 feature.

3. Atomic Data and Equivalent Width Measurements

The atomic data for the Fe I lines used here were taken from the work of the Oxford group (Blackwell et al. 1986) and from O'Brian et al. (1991). Only lines with gf-values certain to 10% or better were adopted from the latter source. In cases where a line was listed in both of the sources, we found that the agreement was generally good, but we adopted the Oxford values in the end. The atomic data for the Fe II lines come from Biemont et al. (1991) and Kroll & Kock (1987) (see also the discussion in Sneden et al. 1991). The atomic data for the [O I] doublet and the O I permitted triplet lines are well known (cf. Lambert 1978). The gf-values for other elements (see Section 6) follow the recommendations given in Sneden et al. (1994), Shetrone (1996) and Kraft et al. (1997), to which the reader if referred for details.

The EWs of the lines were measured using basic IRAF routines. In most cases, we fitted a Gaussian profile to each line, but in the few instances in which a Gaussian fit proved to be poor, we measured the line by direct integration under the continuum. The two methods gave consistent results when tested on lines for which the Gaussian fit was satisfactory. Lines that were badly blended or located on (occasional) bad columns of the CCD chip were not measured. In the spectrum of BD +37 1458, we measured 69 lines of Fe I and 9 lines of Fe II, ranging in EW from 4 to 100 mÅ. In the spectrum of the more metal-poor BD +23 3130, we were able to measure 56 Fe I and 7 Fe II lines, over the same range

of EW. The S/N proved high enough that measurements down to the 2-3 mÅ level can be considered reliable. Table 2 lists the adopted atomic parameters and EWs of all the lines used in this study.

4. Stellar Parameters and Fe Abundances

Analysis of the EWs was done iteratively using the LTE code MOOG (Sneden 1973) together with Kurucz (1992) model atmospheres. The latter were also used by both I98 and B99. Trial values for the stellar parameters (T_{eff} , log g and v_t) were those of I98. The method of analysis closely followed that of the "Lick/Texas" group, and the reader is referred to the last two of a series of papers by that group (Kraft et al. 1997, Sneden et al. 1997) for a more lengthy discussion of the procedures. ³

The ab initio stellar parameters were adjusted so that (1) the stronger Fe I lines gave the same abundance on the average as the weaker lines, (2) the Fe I lines gave an Fe abundance that was on the average independent of excitation potential of the Fe I lines, and (3) the average abundance of Fe based on Fe II lines was the same as that of the Fe I lines (to within 0.02 dex). Because the ratios [Mg/Fe] and [Si/Fe] among metal poor stars are generally positive (and near +0.4 to +0.5), and the solar abundances of Fe, Mg and Si are comparable, the input model should allow for the increased electron density coming from the ionization of Mg and Si. In prior investigations of the Lick/Texas group, that increase was simulated in the input models by adopting a value of [Fe/H] higher than the final iterated value. Thus, for example in the present case, in which the iterated final value of [Fe/H] for BD +37 1458 proved to be -2.31, we adopted an input model abundance of [Fe/H] = -2.0. Since, as proved finally to be the case, [Fe/H] = -2.3 whereas [Mg/Fe] and $[Si/Fe] \sim +0.5$, a compromise input metallicity of -2.0 should allow for an "average" increase in the free electron supply from Mg, Si and Fe by a factor of about 2 (i.e. factors of 3, 3, and 1 for Mg, Si and Fe, respectively). The multiple iteration of the basic parameters following the prescriptions of (1), (2) and (3) above, led to the final adopted values listed in Table 3. Plots of Fe abundance vs Fe I excitation potential (sensitive to the adopted T_{eff}) and Fe abundance vs Fe I line- strength (sensitive to microturbulent velocity v_t) are shown in Figures 1a for BD +21 3130 and 1b for BD +37 1458 for the parameters adopted here.

As a check on the reliability of our procedure in which we simulate the effect on the models of an "overabundance" of Mg and Si relative to Fe by substituting an input model with a "compromise" increase in all three elements, we considered several LTE Kurucz models kindly supplied by Bruce Carney in which actual overabundances of Mg and Si by 0.5 dex relative to Fe were directly incorporated. For example, we compared the effect of the "simulated" ($T_{eff} = 5100 \text{ K}$, $\log g = 2.9$, [Fe/H] = -2.0, [Mg/Fe] = [Si/Fe] = 0.0) and "real" ($T_{eff} = 5100 \text{ K}$, $\log g = 2.9$, [Fe/H] = -2.31, [Mg/Fe] = [Si/Fe] = +0.5) model on the final iterated Fe and O abundances of BD +37 1458, in which the similated values led to [Fe/H] = -2.31. We find that the changes are extremely minor, amounting at most to 0.01 dex in [Fe/H] and 0.05 dex in [O/Fe]. The reason these changes are minor is no doubt a result of the small modifications induced in the free electron supply, since at each reference depth in the continuous opacity τ_{5000} , the

 $^{^{3}}$ We adopt a solar Fe-abundance of log epsilon(Fe) = 7.52. Otherwise all solar abundances adopted here are those of Anders & Grevesse (1989).

change in T_{eff} and N_e amounts to no more than 20 K and 7 percent at the level of the continuum, respectively. This in turn reflects the fact that for the overabundances of Fe, Mg and Si dicussed above, 60 percent or more of the free electron supply is derived from the ionization of H at every optical depth in the atmosphere, and thus is virtually independent of the precise value of the input abundances of these elements.

In Table 3, we list our final values of the stellar parameters along with those adopted by I98 and B99. We obtain values of T_{eff} , derived from our LTE analysis of roughly 60 Fe I lines, that are considerably lower (by 150 to 350K) than those of the other investigations. For comparison purposes, we plot Fe abundance vs Fe I excitation potential and vs Fe I line strength, using our measured Fe I EWs, for the values of T_{eff} and v_t adopted by I98 and B99 (Figures 2a-d). For the B99 paper, the plot corresponds to the adoption of the King (1993) T_{eff} scale. Inspection of these Figures reveals that adoption of the I98 and B99 values of T_{eff} for these two stars leads to unacceptably large slopes and scatter in both the excitation and turbulence plots. Compared with the other two investigations, our values of T_{eff} and log g are lower, but the differences in metallicity, i.e., [Fe/H], are fairly small (≤ 0.2 dex).

As noted above, we obtain log g using the requirement that the Fe abundance derived from the Fe II lines shall closely equal that derived from the Fe I lines. In Table 3, we list the values of $\log \epsilon$ (Fe I) and $\log \epsilon$ (Fe II) from our model parameters for the two stars, and it will be seen that this condition is met to within 0.01 dex. We derive also (Table 3) the mean abundances of Fe I and Fe II for the I98 and B99 model parameters, making use of our EW measurements. These lead to discrepancies in the mean abundance of Fe from Fe I and Fe II of 0.1 to 0.2 dex. We note in the next section that the value of [O/Fe] is somewhat sensitive to the choice of $\log g$. Thus, as an experiment, we examined the Fe ionization equilibrium for an arbitrary 0.3 dex change in $\log g$, having fixed our value of T_{eff} in accordance with the Fe I excitation plot exhibited in Figures 1a and 1b. The changes in $\log \epsilon$ (Fe) from Fe I and Fe II lines are listed in Table 3, and lead to discrepancies in Fe abundance somewhat more than 0.1 dex.

Generally it has been found (cf. Kraft et al. 1997, Sneden et al. 1997, Gonzalez & Wallerstein 1998) that, among globular cluster giants, estimates of surface gravity based on the ionization equilibrium of Fe I and Fe II are in excellent agreement with estimates based on values of the effective temperature, mass and luminosity expected for such stars. Thus, having settled on values of T_{eff} for BD +23 3130 and BD +37 1458, we can check whether our corresponding log g's are consistent with expectation based on stellar evolution, using the color-magnitude arrays of globular clusters. BD +37 1458, for example, has a metallicity ([Fe/H] = -2.3) which is close to that of M92 (Zinn & West 1984, Sneden et al. 1991, Shetrone 1996). Theoretical models of a cluster with this metallicity require log g = 2.7 if T_{eff} = 5100K and the age is 14 Gyr (Straniero & Chieffi 1991); the models of Carbon et al. (1982) for M92 yield log g = 2.8 for this T_{eff} . Our value of log g = 2.9 seems about right. If this star were actually located in M92 it would have M_{Vo} = +1.9 for an assumed distance modulus of $(m - M)_o$ = 14.49 (Djorgovski 1993) and $(B - V)_o$ = +0.62 (Stetson & Harris 1988). The observed (B - V) = +0.60 (Carney et al. 1994). Interstellar reddening in this direction appears to be zero or quite small even though b = 9.8 deg: for five stars selected from the Bright Star Catalog (Hoffleit 1964) within 5 deg of BD +37 1458 and having

 $b \leq 10$ deg, $\langle E(B-V) \rangle = +0.02 \pm 0.03$ (σ). Thus the observed and "predicted" ⁴ M92 colors are quite close. The distance to BD +37 1458 thus becomes 256 pc, which is only slightly beyond the upper limit of the Hipparcos distance plus its estimated error: 173 (+60, -32) pc. The I98 model is also consistent with "membership" in M92, the increase in T_{eff} (from 5100K to 5260K) being compensated by the corresponding increase in log g (from 2.8 to 3.0), and the M_{Vo} derived leads to a distance lying within the error bars of the Hipparcos-based value. The values of T_{eff} and log g assigned to this star by B99 are still larger than the I98 values and again are consistent with the color- magnitude array of M92. Identification of BD +37 1458 as a star consistent with membership in M92 therefore does not help to discriminate which of the models discussed here is correct. But all models do place the star above the main sequence in the subgiant domain.

There are no galactic globular clusters with metallicities as low as [Fe/H] = -2.8, so a direct comparison of BD +23 3130 with globular cluster stars cannot be made. There appear also to be no available theoretical isochrones corresponding to clusters with metallicities below that of M92. Examination of the Straniero and Chieffi isochrones with respect to [Fe/H] suggests that subgiant and giant branches crowd more closely together as metallicity decreases; thus extrapolation toward a metallicity as low as [Fe/H] = -2.8 is a dangerous procedure. Nevertheless, we estimate that, relative to BD +37 1458, BD +23 3130 should be ~ 0.05 mag bluer in (B-V) because of its reduced metallicity and ~ 0.10 mag redder because of its reduced T_{eff} , and thus if $(B-V)_o = 0.60$ for the former star, $(B-V)_o = 0.65$ for the latter. The observed (B-V) = 0.64 (Carney et al. 1994). Once again we find $< E(B-V) > = 0.01 \pm 0.07$ from the five nearest stars in the Bright Star Catalog, so interstellar reddening is quite small or vanishing. However, because in color-magnitude diagrams, cluster giant branches are extremely steep, we suggest that using estimates of color to derive values of M_V is an unwise procedure. The best we can say is that we expect BD +23 3130 to have a lower log g than BD +37 1458, as we see from our spectroscopic determination.

In Figures 3a and 3b, we synthesize three Fe I lines of similar intermediate excitation (2.4 to 2.6 eV) and differing strengths in the spectral region λ 6134 Å to λ 6140 Å, using our parameters and those of I98 and B99. The Hamilton spectra, binned by two pixels (= effective spectral resolution) are shown as dots. The parameters adopted by I98 and B99 produce synthesized lines that are too weak compared with the observed spectra. Obviously the discrepancies could be reduced simply by increasing the Fe abundance, but such a change would introduce a serious discordance between models and observations for lines of higher and lower excitation, as seems clear from inspection of Figures 2a-d.

 $^{^4}$ From the same source, one finds $< E(B-V) > = +0.01 \pm 0.13$ for the five stars nearest to BD +37 1458, and having D > 100 pc. Stars fainter than those in the Bright Star Catalog, and close to BD +37 1458, are found in the Hipparchos Survey (1997). There are 3 stars (a K0 giant, a K0 supergiant, and a main-sequence A2 star) between $l = 171^o$ and 175^o , having distances greater than 150 pc and $b < 8^o$. For these $< E(B-V) > = 0.01 \pm 0.03$. Unfortunately the spectral types are those assigned by the Draper Catalog; MK classifications are unknown. In the direction of BD +37 1458, the dust reddening maps (Schlegel et al. 1998) lead to E(B-V) = 0.28. Evidently some dust clouds are located in a region beyond BD +37 1458.

5. Oxygen Abundances

Using the same techniques we employed to create Figures 3a and 3b, we show in Figures 4a,b and 5a-d the spectral region surrounding the λ 6300 [O I] line in BD +23 3130 and BD +37 1458, respectively. Again our observed Lick spectra (binned by 2) are shown as dots. In each figure, the Fe abundance was held constant while the O abundance was changed to create plots (thin lines) for values of [O/Fe] = 0.0, +0.5, +1.0 and +1.5. The model parameters and Fe abundances are those corresponding to each individual investigation discussed in this paper.

Turning first to the spectrum of BD +23 3130, we see that the present synthesis gives a satisfactory representation of the Fe I lines at $\lambda\lambda$ 6297.8 Å, 6301.5 Å and 6302.5 Å, and leads to an estimated oxygen abundance of $[O/Fe] = +0.35 \pm 0.2$ (est. error, based on the S/N). However, the $[O\ I]$ line is so weak (we estimate EW ~ 1 mÅ) that the quoted [O/Fe]-value may be an upper limit, in which case the true oxygen abundance is even smaller than [O/Fe] = +0.35. The I98 model produces Fe I lines that are much too weak, but corresponds to an estimated oxygen abundance of $[O/Fe] = +0.7 \pm 0.2$. Neither model comes close, however, to the value [O/Fe] = +1.17 obtained by I98 from synthesis of the OH features. Thus for this star, there is a serious discrepancy between the oxygen abundances derived from $[O\ I]$ and OH, even if we adopt the parameters T_{eff} , log g, v_t and [Fe/H] suggested by I98.

The situation with respect to BD +37 1458 is less decisive. The synthesis using the present parameters leads to a satisfactory representation of the three Fe I lines listed in the preceding paragraph, and the corresponding oxygen abundance is $[O/Fe] = +0.5 \pm 0.2$. The I98 model produces Fe I lines at $\lambda\lambda$ 6297.8 Å and 6301.5 Å that are much too weak, although the modelling of the remaining Fe I line is satisfactory. The corresponding oxygen abundance is $[O/Fe] = +0.75 \pm 0.2$, a value reasonably close to the value [O/Fe] = +0.97 obtained by I98 from the OH features. This star was also considered by B99, who found [O/Fe] = 0.875 and 0.83, based on modelling the OH features, using the Carney (1983) and King (1993) T_{eff} scales, respectively. These values of [O/Fe] are statistically indistiguish- able from the value of [O/Fe] we derive from the [O I] line, using their choices of the basic parameters. However, as we have seen, these models give a poor representation of the Fe I lines (Figures 3a,3b), and do not satisfy the requirements of the Fe I excitation and turbulence plots (Figures 2a-d).

We may also explore the changes in oxygen abundance derived from OH that would be induced if I98 and B99 had adopted the values of T_{eff} preferred by our analysis. According to B99, an increase in T_{eff} by 100 K increases the derived O from OH by +0.16 dex. But it also increases Fe by ~ 0.07 dex. So the net increase in [O/Fe] is about 0.09 dex. If I98 had adopted our T_{eff} for BD +37 1458 their [O/Fe] would have gone down by ~ 0.15 dex. In the case of BD +23 3130, the reduction would be ~ 0.25 dex.

6. Other Elements

In Table 4 and 5 we list, along with the determinations of [O/Fe] cited in Section 5, abundances [el/Fe] for Na, the alpha elements Mg, Si, Ca and Ti, and the Fe-peak element Ni for the two stars studied here. In both Tables, the [el/Fe]-ratios are based on the EWs determined in this study. The Tables differ in that the adopted Fe abundances of Table 4 are taken as the Fe I abundances we derive using these EWs and the model parameters (T_{eff} , log g) used by I98 and B99, whereas the Fe abundances of

Table 5 are those actually adopted by I98 and B99. We list also in these Tables the mean [el/Fe]-ratios found by McWilliam et al. (1995) for a large sample of metal-poor stars having [Fe/H] < -2.0.

At any given [Fe/H], the scatter in [el/Fe]-ratios in the McWilliam et al. (1995) sample is typically ~ 0.2 dex for stars more metal-rich than [Fe/H] =-3.2. Thus we see from inspection of Tables 4 and 5 that almost all models give [el/Fe]-ratios for BD +37 1458 and BD +23 3130 that are in reasonable agreement with the mean [el/Fe]-ratios of the McWilliam et al. (1995) sample. The only significant departures seem to be those of the I98 models tabulated in Table 5. For these the [el/Fe]-ratios appear to be rather large, and the values for Na and Ni are particularly uncomfortable. However, this departure is much reduced if we use the (mean) Fe-abundances we derive from the present set of EWs and the I98 model parameters, rather than the Fe abundances actually adopted by I98. Except for these two models of Table 5, the [el/Fe] ratios for the " α elements", Mg, Si and Ca are close to their "normal" expected values of $\sim +0.4$ to +0.6 [cf., e.g., $[\alpha/Fe]$ -ratios in M15 giants (Sneden et al. 1997).].

7. Conclusions

In an analysis of the OH bands (λ 3100 Å) of 23 presumed subdwarfs, I98 found that the oxygen abundances were generally higher than the traditionally accepted values that had been determined from the analysis of the [O I] doublet in the spectra of low-metallicity giants. Similar conclusions have also been reached by B99, again from analysis of the OH bands in subdwarfs. The differences increase with decreasing metallicity, and reach $\sim+0.6$ dex as [Fe/H] approaches -3.0. In particular, the two highest [O/Fe]-ratios in the I98 sample were those found in BD +37 1458 and BD + 23 3130, for which [O/Fe] = +0.97 and +1.17 for [Fe/H] = -2.40 and -2.90, respectively. In their analysis of the former star, B99 found a similar high value of [O/Fe] = 0.87 or 0.83, depending on the choice of temperature scale.

Atmospheric modelling of very metal-poor ([Fe/H < -2) subdwarfs shows that the [O I]-doublet, even for [O/Fe]-ratios as high as +1.0, practically "disappears": the EW of the stronger member of the pair (λ 6300A) approaches 1.0 mÅ or less. However, examination of the I98 sample indicates that the two stars discussed above have surface gravities more like subgiants than subdwarfs. These two stars thus presented the possibility that the EWs of the λ 6300 Å line of [O I] might be measureable in spectra having sufficiently high S/N, and thus provide a check on the oxygen abundances derived from the OH feature.

Thus, on the basis of high resolution (R = 50000), high S/N (~250) echelle spectra of BD +23 3130 and BD +37 1458, we have determined abundances [Fe/H], and [el/Fe]-ratios for Na, Ni, and the traditional alpha elements Mg, Si, Ca and Ti. We conducted a full-scale abundance analysis based on the EWs of about 60 Fe I and 7-9 Fe II lines, from which we determined from LTE models the appropriate values of T_{eff} , log g, [Fe/H] and v_t , independent of considerations based on the calibration of color scales. We determined oxygen abundances from synthetic spectra of the region encompassing the [O I] line at λ 6300 Å. Our conclusions are these:

- (1) Based on the ionization equilibrium of Fe, we find that these two stars are indeed subgiants, with surface gravities somewhat lower than those adopted by I98 and B99.
 - (2) Our values of T_{eff} are also lower than those obtained by I98 and B99, by amounts between ${\sim}150$

and 300K. Our [Fe/H] values are nevertheless within \sim 0.2 dex of those determined by I98 and B99. The metallicity of BD +37 1458 is essentially the same as that of M92; all models are in reasonable agreement with the assumption that this star is a surrogate for an M92 star lying on the steep subgiant branch of that cluster. The metallicity of +23 3130 is lower than that of any known galactic globular cluster.

- (3) Except for two models listed in Table 5, all investigations lead to plausible [el/Fe]-ratios for alpha elements, Na and Ni, when compared with those found for metal-poor stars by McWilliam et al. (1995).
- (4) Our synthetic spectra of the region of the [O I] line at λ 6300 Å lead to the traditional oxygen abundances of [O/Fe] = $+0.35 \pm 0.2$ for BD +23 3130 and $+0.50 \pm 0.2$ for BD +37 1458. The [O/Fe]-value quoted for BD +23 3130 may be an upper limit.
- (5) Use of our Fe I EWs leads to a fairly low value of [O/Fe] = +0.7 in the case of BD +23 3130, even if we adopt the parameters of I98. For the other star, an [O/Fe]-ratio closer to the value derived from the OH feature is found if the parameters adopted by I98 and B99 are adopted. These parameters, however, yield a poor representation of the Fe I features in this star, as do the parameters adopted by I98 for BD +23 3130.
- (6) A discrepancy therefore remains among these two stars between the [O/Fe]-ratio derived from [O I] and the OH feature. This is of some significance especially when one realizes that these two stars have the highest [O/Fe]-ratios among the stars considered by I98. The origin of these differences remains unclear.
- (7) The procedures adopted here are identical with those previously employed (e.g., Sneden et al. 1997, Kraft et al. 1997) in the analysis of the spectra of globular cluster and halo field giants and subgiants. In these studies, analysis of the Fe I and Fe II line spectra is a basic requirement in the determination of atmospheric parameters.
- (8) The results obtained here suggest that it is too early to conclude that the oxygen abundances of old, metal-poor stars need to be revised drastically upward. We suggest that input models for such stars need to be examined in the light of a full LTE analysis of the Fe I and Fe II spectrum, before values of T_{eff} , log g, v_t and [Fe/H] are assigned.

We are indebted to C. Sneden for use of his MOOG code, and have benefitted from useful conversations with R. Peterson. We are especially grateful to Bruce Carney for supplying us with several α -enhanced Kurucz model atmospheres and for reading and commenting on a preliminary version of this manuscript. This research has been supported by NSF Grant AST 96-18351, which we greatly appreciate.

Table 1. Log of Observations.

	BD +23 3130	BD +37 1458
UT Date	8 Aug 1998	31 Oct 1998
Exposure	3600 s	3600 s
V	8.95	8.92
B-V	0.64	0.60

Table 2. Line Measurements.

Wavelength (Å)	E.P. (eV)	$\log(gf)$	EW (mÅ) BD +37 1458	EW (mÅ) BD +23 3130	Ref
Fe I					
4531.15	1.49	-2.155	58.2	44.5	1d
4592.66	1.56	-2.449	45.4	29.4	1d
4602.01	1.61	-3.154	12.1	7.6	1d
4602.94	1.49	-2.208	54.8	45.3	1d
4643.46	3.64	-1.147	7.5	_	2
4647.43	2.94	-1.351	23.6	13.4	2
4733.60	1.49	-2.987	24.3	14.0	1d
4736.77	3.20	-0.752	36.7	_	2
4786.81	3.00	-1.606	12.4	7.6	2
4789.65	3.53	-0.957	15.9	_	2
4871.32	2.85	-0.362	69.6	54.8	2
4872.14	2.87	-0.567	60.6	45.3	2
4890.75	2.86	-0.394	72.6	54.8	2
4891.49	2.84	-0.111	84.5	_	2
4918.99	2.85	-0.342	74.5	59.5	2
4938.81	2.86	-1.077	36.4	24.6	2
4939.69	0.86	-3.340	38.2	31.2	1b
4994.13	0.91	-3.080	48.8	38.5	1b
5006.12	2.82	-0.615	62.3	45.5	2
5028.13	3.56	-1.122	9.0	_	2
5041.07	0.95	-3.086	49.2	37.3	2
5044.21	2.85	-2.017	9.0	_	2
5048.44	3.94	-1.029	5.1	_	2
5049.82	2.27	-1.355	56.7	44.1	2
5051.64	0.91	-2.795	63.9	54.1	1b
5068.77	2.93	-1.041	_	22.2	2
5079.23	2.20	-2.067	30.6	20.1	1b
5079.74	0.99	-3.220	38.1	28.1	1b
5083.34	0.96	-2.958	52.6	42.4	1b
5107.45	0.99	-3.087	43.8	34.0	1b
5107.65	1.56	-2.418	44.6	33.8	1d
5123.72	1.01	-3.068	44.4	35.2	1b
5127.36	0.91	-3.307	37.3	30.6	1b

Table 2. (continued)

Wavelength (Å)	E.P. (eV)	$\log(gf)$	EW (mÅ) BD +37 1458	EW (mÅ) BD +23 3130	Ref
5151.92	1.01	-3.322	32.2	22.1	1b
5191.45	3.03	-0.551	54.9	37.6	2
5192.34	2.99	-0.421	60.8	45.8	2
5198.71	2.22	-2.135	25.2	16.4	1c
5216.28	1.61	-2.150	56.9	43.8	1d
5217.39	3.20	-1.162	21.9	13.3	2
5232.94	2.94	-0.057	82.7	67.8	2
5242.49	3.62	-0.967	_	6.0	2
5247.05	0.09	-4.946	11.2	_	1a
5288.53	3.68	-1.508	3.9	_	2
5307.37	1.61	-2.987	18.6	11.4	1d
5367.47	4.42	0.443	_	16.7	2
5383.37	4.31	0.645	_	28.1	2
5397.13	0.91	-1.993	96.8	_	1b
5405.78	0.99	-1.844	98.3	_	1b
5434.53	1.01	-2.122	88.9	_	1b
5501.46	0.95	-3.046	51.2	40.1	2
5506.78	0.99	-2.797	60.9	51.0	1b
5701.55	2.56	-2.216	11.1	6.1	1f
6065.49	2.61	-1.530	35.5	22.9	1f
6136.62	2.45	-1.400	51.2	34.2	1e
6137.70	2.59	-1.403	45.2	30.0	1f
6173.34	2.22	-2.880	8.0	_	1e
6219.29	2.20	-2.433	16.5	9.9	1c
6230.73	2.56	-1.281	54.5	37.4	1f
6246.32	3.59	-0.877	19.8	9.9	2
6252.56	2.40	-1.687	38.9	28.7	1c
6265.14	2.18	-2.550	15.9	9.9	1e
6297.80	2.22	-2.740	11.0	_	$1c^{a}$
6322.69	2.59	-2.426	7.9	_	1f
6358.69	0.86	-4.468	7.6	_	1b
6411.65	3.64	-0.717	_	13.1	2
6421.36	2.28	-2.027	33.6	18.6	1e
6430.85	2.18	-2.006	39.4	25.2	1c
6494.99	2.40	-1.273	61.2	48.9	1e

Table 2. (continued)

Wavele	ength (Å)	E.P. (eV)	$\log(gf)$	EW (mÅ) BD +37 1458	EW (mÅ) BD +23 3130	Ref
	6593.88	2.43	-2.422	11.9	6.1	1c
	6677.99	2.68	-1.418	42.3	27.5	2
	6945.21	2.42	-2.482	_	6.7	1c
	6750.15	2.42	-2.621	8.0	_	1e
	6945.21	2.42	-2.482	11.4	_	1c
	6978.86	2.48	-2.500	10.9	_	1c
	7511.02	4.16	0.099	32.9	19.7	2
Fe II						
	4555.88	2.83	-2.290	33.2	28.7	3
	4576.34	2.84	-2.822	13.4	10.6	4
	4582.83	2.84	-3.094	10.9	6.2	4
	4620.52	2.83	-3.079	_	5.7	4
	4923.92	2.89	-1.240	77.0	_	3
	5197.58	3.23	-2.233	25.6	19.6	4
	5234.63	3.22	-2.151	28.5	23.0	4
	5316.62	3.15	-1.850	44.9	35.7	3
	6247.56	3.89	-2.329	6.2	_	4
	6456.39	3.90	-2.075	10.1	_	4
Na I						
	5688.21	2.10	-0.370	8.7	_	5
	5889.96	0.00	0.110	165.1	128.7	6
	5895.94	0.00	-0.190	152.0	108.8	6
Mg I						
	4730.03	4.33	-2.310	3.6	_	7
	5172.70	2.71	-0.320	292.8	188.7	8^{a}
	5183.42	2.72	-0.080	353.2	203.7	8^{a}
	5528.42	4.35	-0.360	85.5	56.8	7
	5711.09	4.33	-1.730	18.3	8.3	7

Table 2. (continued)

Wavel	ength (Å)	E.P. (eV)	$\log(gf)$	EW (mÅ) BD +37 1458	EW (mÅ) BD +23 3130	Ref
Si I						
	5701.12	4.93	-2.050	2.9	_	9
	5708.41	4.93	-1.470	_	3.4	9
	5948.55	5.08	-1.230	9.2	6.5	9
	7415.96	5.61	-0.710	11.5	5.3	9
	7423.52	5.61	-0.780	13.4	7.7	9
Ca I						
	4578.56	2.52	-0.700	13.5	6.6	10
	5261.71	2.52	-0.580	18.8	9.9	10
	5349.47	2.71	-0.310	20.2	11.2	10
	5581.97	2.52	-0.560	25.0	9.5	10
	5588.76	2.52	0.360	62.8	37.4	10
	5590.12	2.52	-0.570	18.7	9.7	10
	5857.46	2.93	0.240	35.3	21.8	10
	6122.23	1.89	-0.320	72.0	46.8	11
	6161.30	2.52	-1.270	4.2	_	10
	6162.18	1.90	-0.090	87.5	61.0	11
	6163.75	2.52	-1.290	7.5	_	10
	6166.44	2.52	-1.200	10.6	_	10
	6169.04	2.52	-0.800	15.6	8.9	10
	6169.56	2.52	-0.480	21.5	12.3	10
	6439.08	2.52	0.390	66.7	42.8	10
	6455.60	2.52	-1.290	6.1	_	10
	6499.65	2.52	-0.820	15.0	_	10
Ti I						
	4555.49	0.85	-0.490	8.0	5.5	12^{a}
	4617.28	1.75	0.390	7.7	5.6	12
	4623.10	1.74	0.110	4.7	_	12
	4681.92	0.05	-1.070	18.7	10.5	12
	4840.88	0.90	-0.510	10.2	5.6	12
	4885.09	1.89	0.360	5.0	_	12
	4991.07	0.84	0.380	43.6	32.5	12
	4999.51	0.83	0.250	38.2	24.8	12

Table 2. (continued)

Wavelength (Å)	E.P. (eV)	$\log(gf)$	EW (mÅ) BD +37 1458	EW (mÅ) BD +23 3130	Ref
5020.03	0.84	-0.410	13.7	8.5	12
5024.85	0.82	-0.600	9.5	5.6	12
5064.66	0.05	-0.990	22.8	15.5	12
5173.75	0.00	-1.120	19.0	11.4	12^{a}
5210.39	0.05	-0.880	27.4	17.5	12
6258.71	1.46	-0.270	5.0	_	12
6261.11	1.43	-0.480	4.0	_	12
Ti II					
4708.67	1.24	-2.210	13.5	9.5	12
5154.08	1.57	-1.920	22.1	16.5	12
5185.91	1.89	-1.350	21.2	18.6	12
5226.54	1.57	-1.300	47.0	33.3	12
5336.79	1.58	-1.700	26.9	19.6	12
Ni I					
4756.52	3.48	-0.340	_	5.3	13
4829.03	3.54	-0.330	7.1	_	13
4831.18	3.61	-0.420	6.2	_	13
4904.42	3.54	-0.170	_	5.3	13
5017.58	3.54	-0.080	10.2	6.7	13
5081.12	3.85	0.300	14.6	7.5	13
5476.92	1.83	-0.890	60.3	46.9	13
5754.67	1.93	-2.330	6.4	_	13
6643.65	1.68	-2.300	10.6	6.7	13
6767.78	1.83	-2.170	12.1	6.8	13

^aLine not used in abundance analysis.

References for Table 2.

(1) "Oxford" group: (a) Blackwell et al. 1979a, (b) Blackwell et al. 1979b, (c) Blackwell et al. 1982a, (d) Blackwell et al. 1980, (e) Blackwell et al. 1982b, (f) Blackwell et al. 1982c; (2) O'Brian et al. 1991; (3) Kroll & Kock 1987; (4) Biemont et al. 1991; (5) Lambert & Warner 1968; (6) Weise et al. 1969; (7) Fuhrmann et al. 1995; (8) Thevenin 1989; (9) Garz 1973; (10) Smith & Raggett 1981; (11) Weise & Martin 1980; (12) Martin et al. 1988; (13) Fuhr et al. 1988.

Table 3. Atmospheric Parameters.

	T_{eff}	$\log g$	[Fe/H]	v_t	$\log \epsilon (\text{Fe I})$	$\sigma(\text{Fe I})$	$\log \epsilon (\mathrm{Fe\ II})$	$\sigma(\text{Fe II})$
BD +23 3130								
This Paper	$4850~\mathrm{K}$	2.00	-2.84	1.35	4.69	0.04	4.68	0.08
This Paper, log g down	$4850~\mathrm{K}$	1.70	-2.84	1.35	4.70	0.04	4.58	0.08
This Paper, log g up	$4850~\mathrm{K}$	2.30	-2.84	1.35	4.67	0.04	4.78	0.08
I98	$5130~\mathrm{K}$	2.50	-2.90	1.00	5.02	0.09	4.89	0.08
BD +37 1458								
This Paper	$5100~\mathrm{K}$	2.90	-2.31	1.40	5.21	0.04	5.21	0.08
This Paper, log g down	$5100~\mathrm{K}$	2.60	-2.31	1.40	5.22	0.04	5.11	0.07
This Paper, log g up	$5100~\mathrm{K}$	3.20	-2.31	1.40	5.20	0.04	5.32	0.08
I98	$5260~\mathrm{K}$	3.00	-2.40	1.00	5.47	0.10	5.30	0.08
B99, K93 scale	$5554~\mathrm{K}$	3.62	-2.06	1.50	5.64	0.09	5.48	0.07
B99, C83 scale	$5408~\mathrm{K}$	3.41	-2.14	1.50	5.50	0.07	5.40	0.08

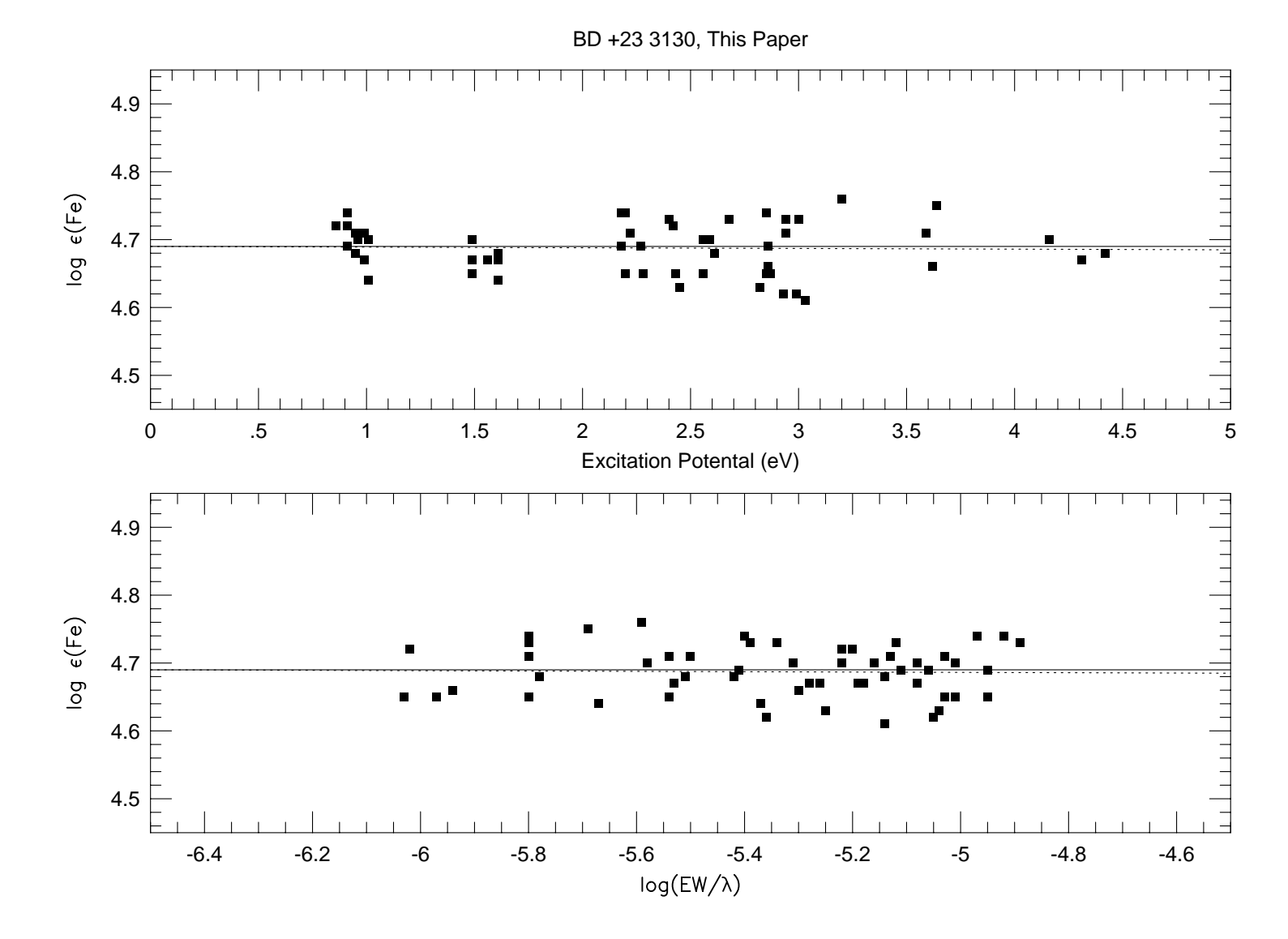
Table 4. Derived Abundances.

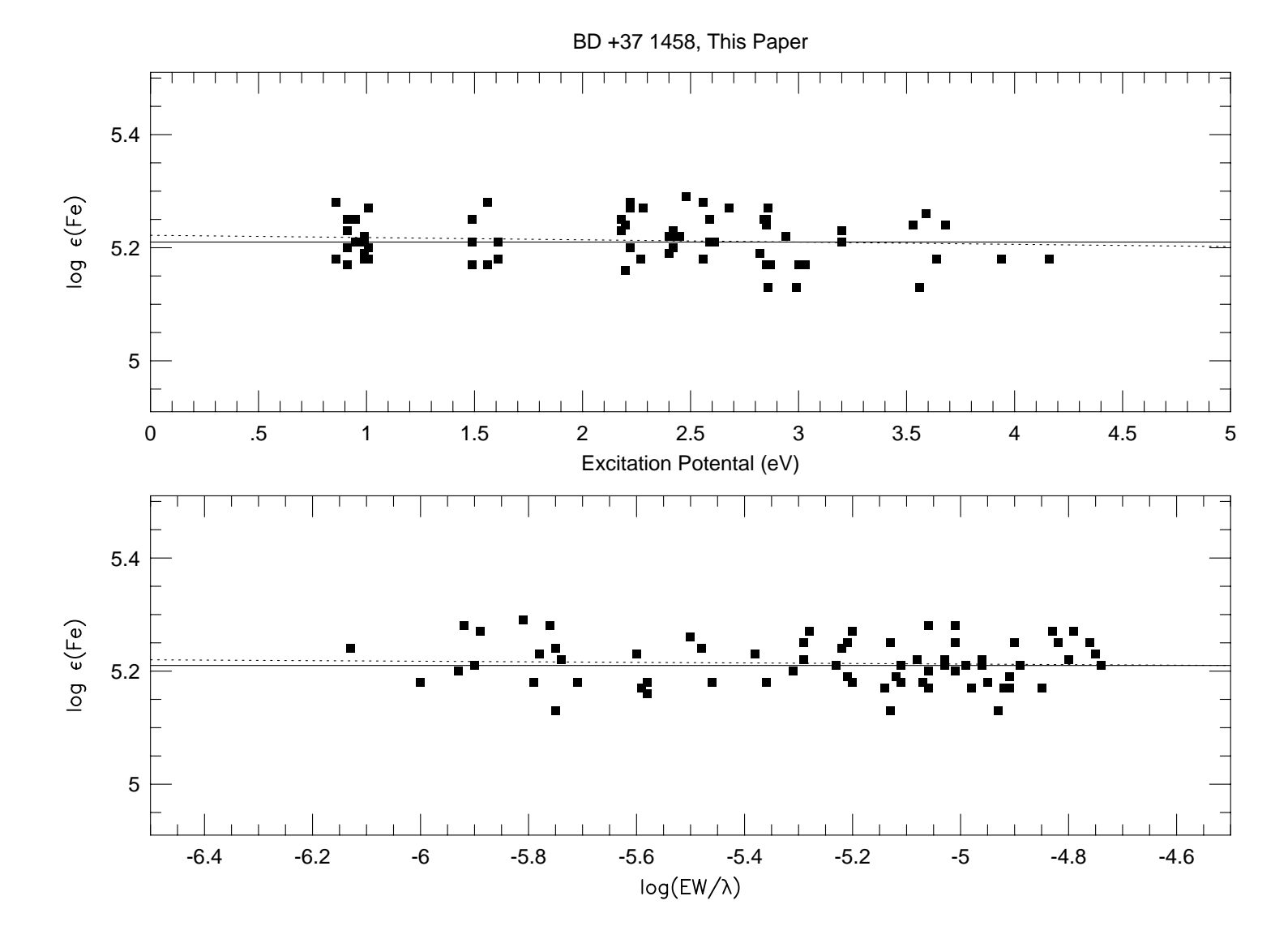
	BD +23 :	3130		BD ±	37 1458		McWilliam
	This Paper	I98	This Paper	I98	B99-K93	B99-C83	et al. 1995
$\log \epsilon(\text{Fe I})$	4.69	5.02	5.21	5.47	5.64	5.50	
$[Fe/H]_{FeI}$	-2.83	-2.50	-2.31	-2.05	-1.88	-2.02	
σ	0.04	0.09	0.04	0.10	0.09	0.07	
$\log \epsilon (\text{Fe II})$	4.68	4.89	5.21	5.30	5.48	5.40	
$[Fe/H]_{FeII}$	-2.84	-2.63	-2.31	-2.22	-2.04	-2.12	
σ	0.08	0.08	0.08	0.08	0.07	0.08	
$\log \epsilon([O\ I])$	6.45	6.73	7.12	7.28	7.67	7.49	
[O/Fe]	0.35	0.30	0.50	0.40	0.62	0.58	
σ	0.20	0.20	0.20	0.20	0.20	0.20	
$\log \epsilon(\text{Na I})$	3.54	3.86	4.07	4.27	4.32	4.24	
[Na/Fe]	0.05	0.04	0.06	0.00	-0.12	-0.06	~ 0.1
σ	0.06	0.09	0.10	0.16	0.13	0.11	
$\log \epsilon(Mg I)$	5.34	5.54	5.83	5.99	6.04	5.98	
[Mg/Fe]	0.60	0.47	0.57	0.47	0.35	0.43	0.42
σ	0.06	0.18	0.13	0.19	0.16	0.15	
$\log \epsilon(\text{Si I})$	5.43	5.55	5.87	5.94	6.05	6.00	
[Si/Fe]	0.72	0.51	0.64	0.45	0.39	0.48	0.50
σ	0.17	0.19	0.12	0.14	0.13	0.12	
$\log \epsilon(\text{Ca I})$	3.98	4.17	4.52	4.67	4.77	4.70	
[Ca/Fe]	0.52	0.38	0.54	0.43	0.36	0.43	0.43
σ	0.09	0.12	0.12	0.16	0.14	0.13	
$\log \epsilon(\mathrm{Ti})$	2.34	2.65	2.87	3.05	3.32	3.18	
$[Ti/Fe]_{Ti}$	0.19	0.17	0.20	0.12	0.22	0.22	0.32
σ	0.10	0.12	0.09	0.13	0.12	0.11	
$\log \epsilon(\text{Ni I})$	3.46	3.72	3.96	4.13	4.34	4.22	
[Ni/Fe]	0.05	-0.02	0.03	-0.06	-0.02	0.00	~ 0.0
σ	0.06	0.11	0.08	0.15	0.15	0.12	

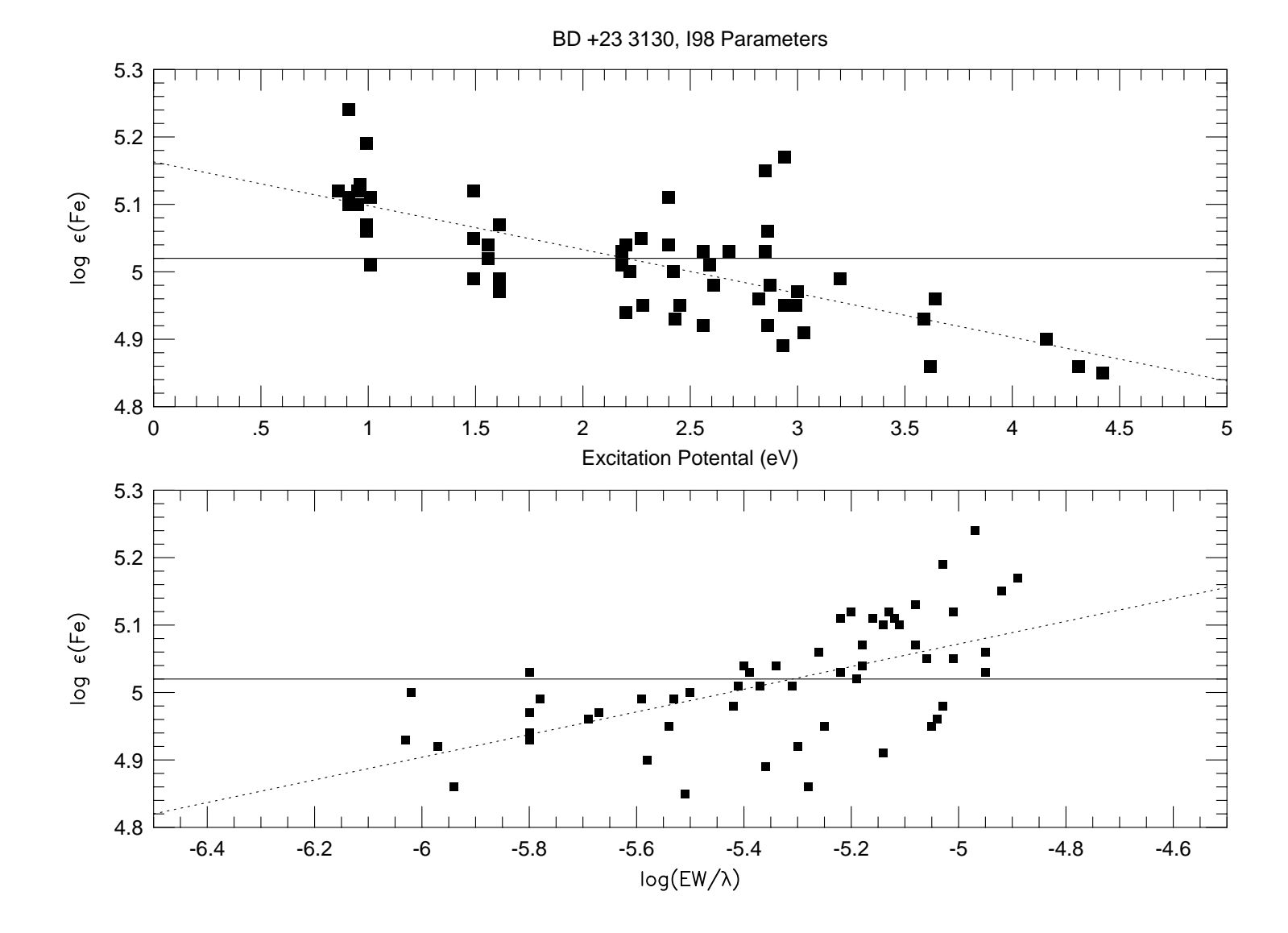
Table 5. Derived Abundances.

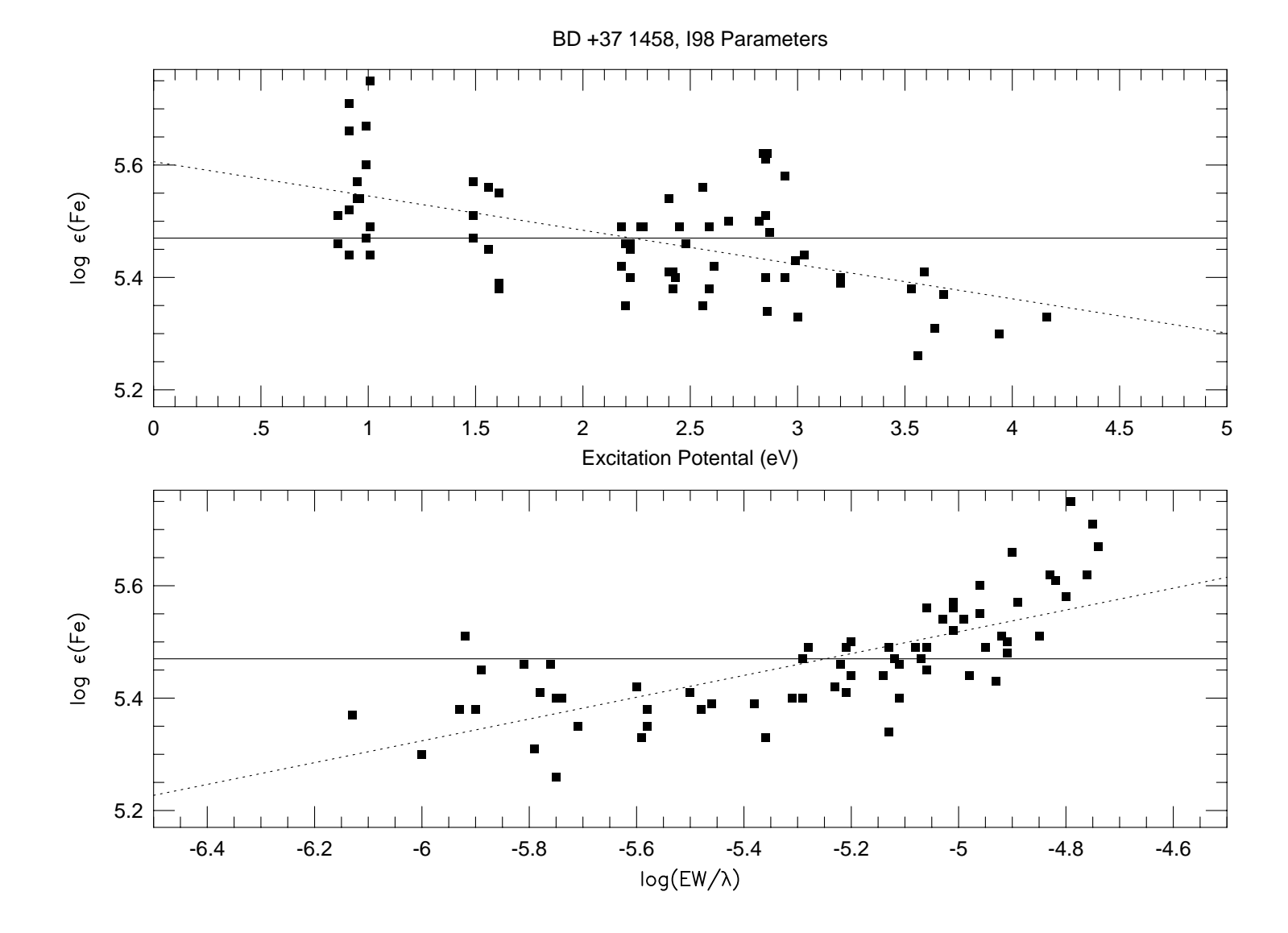
	BD +23 3	3130		BD +	37 1458		McWilliam
	This Paper	I98	This Paper	I98	В99-К93	B99-C83	et al. 1995
$\log \epsilon (\text{Fe I})$	4.69	4.62	5.21	5.12	5.46	5.38	
$[Fe/H]_{FeI}$	-2.83	-2.90	-2.31	-2.40	-2.06	-2.14	
$\log \epsilon (\text{Fe II})$	4.68	4.62	5.21	5.12	5.46	5.38	
$[Fe/H]_{FeII}$	-2.84	-2.90	-2.31	-2.40	-2.06	-2.14	
$\log \epsilon([O\ I])$	6.45	6.73	7.12	7.28	7.67	7.49	
[O/Fe]	0.35	0.70	0.50	0.75	0.80	0.70	
σ	0.20	0.20	0.20	0.20	0.20	0.20	
$\log \epsilon(\text{Na I})$	3.54	3.86	4.07	4.27	4.32	4.24	
[Na/Fe]	0.05	0.44	0.06	0.35	0.06	0.06	~ 0.1
σ	0.05	0.02	0.09	0.12	0.09	0.09	
$\log \epsilon(Mg I)$	5.34	5.54	5.83	5.99	5.98	6.04	
[Mg/Fe]	0.60	0.87	0.57	0.82	0.53	0.55	0.42
σ	0.05	0.16	0.12	0.16	0.13	0.13	
$\log \epsilon(\text{Si I})$	5.43	5.55	5.87	5.94	6.05	6.00	
[Si/Fe]	0.72	0.91	0.64	0.80	0.57	0.60	0.50
σ	0.17	0.17	0.11	0.10	0.10	0.10	
$\log \epsilon(\text{Ca I})$	3.98	4.17	4.52	4.67	4.77	4.70	
[Ca/Fe]	0.52	0.78	0.54	0.78	0.54	0.55	0.43
σ	0.08	0.08	0.11	0.13	0.11	0.11	
$\log \epsilon(\mathrm{Ti})$	2.34	2.65	2.87	3.05	3.32	3.18	
$[Ti/Fe]_{Ti}$	0.19	0.57	0.20	0.47	0.40	0.34	0.32
σ	0.09	0.07	0.08	0.09	0.09	0.08	
$\log \epsilon(\text{Ni I})$	3.46	3.72	3.96	4.13	4.34	4.22	
[Ni/Fe]	0.05	0.38	0.03	0.29	0.16	0.12	~ 0.0
σ	0.05	0.07	0.07	0.11	0.12	0.10	

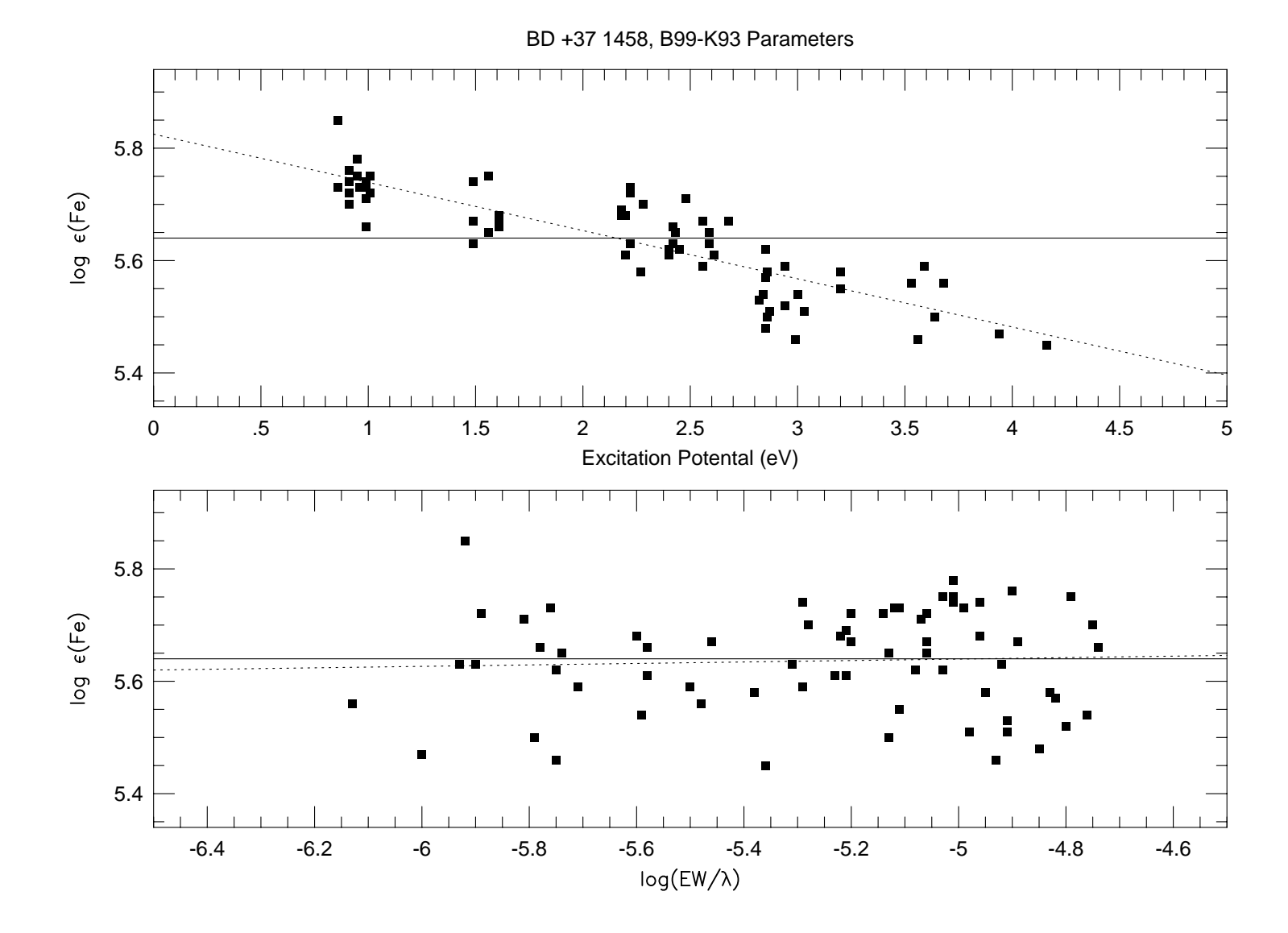
- Figure 1a. Plots of abundance vs. excitation potential and line strength for the individual Fe I lines of BD +23 3130 using the stellar parameters adopted by this paper.
- Figure 1b. Same as Figure 1a, expect for BD +37 1458.
- Figure 2a. Same as Figure 1a, except using the parameters of I98.
- Figure 2b. Same as Figure 1b, except using the parameters of I98.
- Figure 2c. Same as Figure 1b, except using the parameters of B99 (King 1993 scale).
- Figure 2d. Same as Figure 1b, except using the parameters of B99 (Carney 1983 scale).
- Figure 3a. Observed and synthetic spectra of Fe I lines in the λ 6137 Å region of BD +23 3130. The dots are the observed data points (binned 2X), and the lines are the synthetic spectra using the stellar parameters adopted by this paper (solid) and by I98 (dotted).
- Figure 3b. Same as Figure 3a, except for BD +37 1458. The lines are the synthetic spectra for the stellar parameters adopted by this paper (solid), I98 (dotted), B99 using the King 1993 scale (short dash), and B99 using the Carney 1983 scale (long dash).
- Figure 4a. Observed and synthetic spectra for the λ 6300 Å region of BD +23 3130. The dots are the observed data points (binned 2x) and the lines are the synthetic spectra for the stellar parameters adopted by this paper for [O/Fe] = +0.0, +0.5, +1.0 and +1.5.
- Figure 4b. Same as Figure 4a, except for BD +37 1458.
- Figure 5a. Same as Figure 4a, except using the parameters of I98.
- Figure 5b. Same as Figure 4b, except using the parameters of I98.
- Figure 5c. Same as Figure 4b, except using the parameters of B99 (King 1993 scale).
- Figure 5d. Same as Figure 4b, except using the parameters of B99 (Carney 1983 scale).

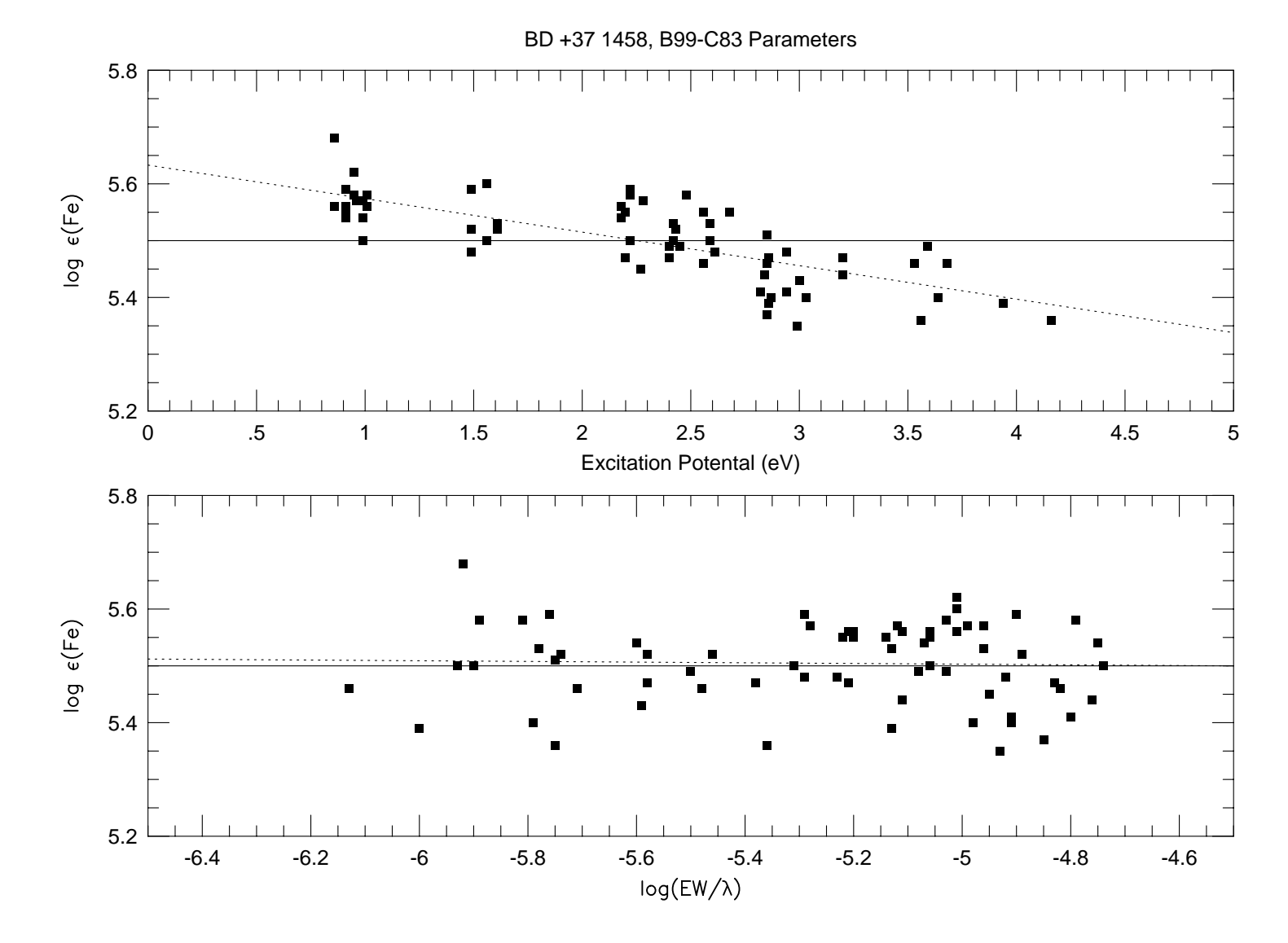


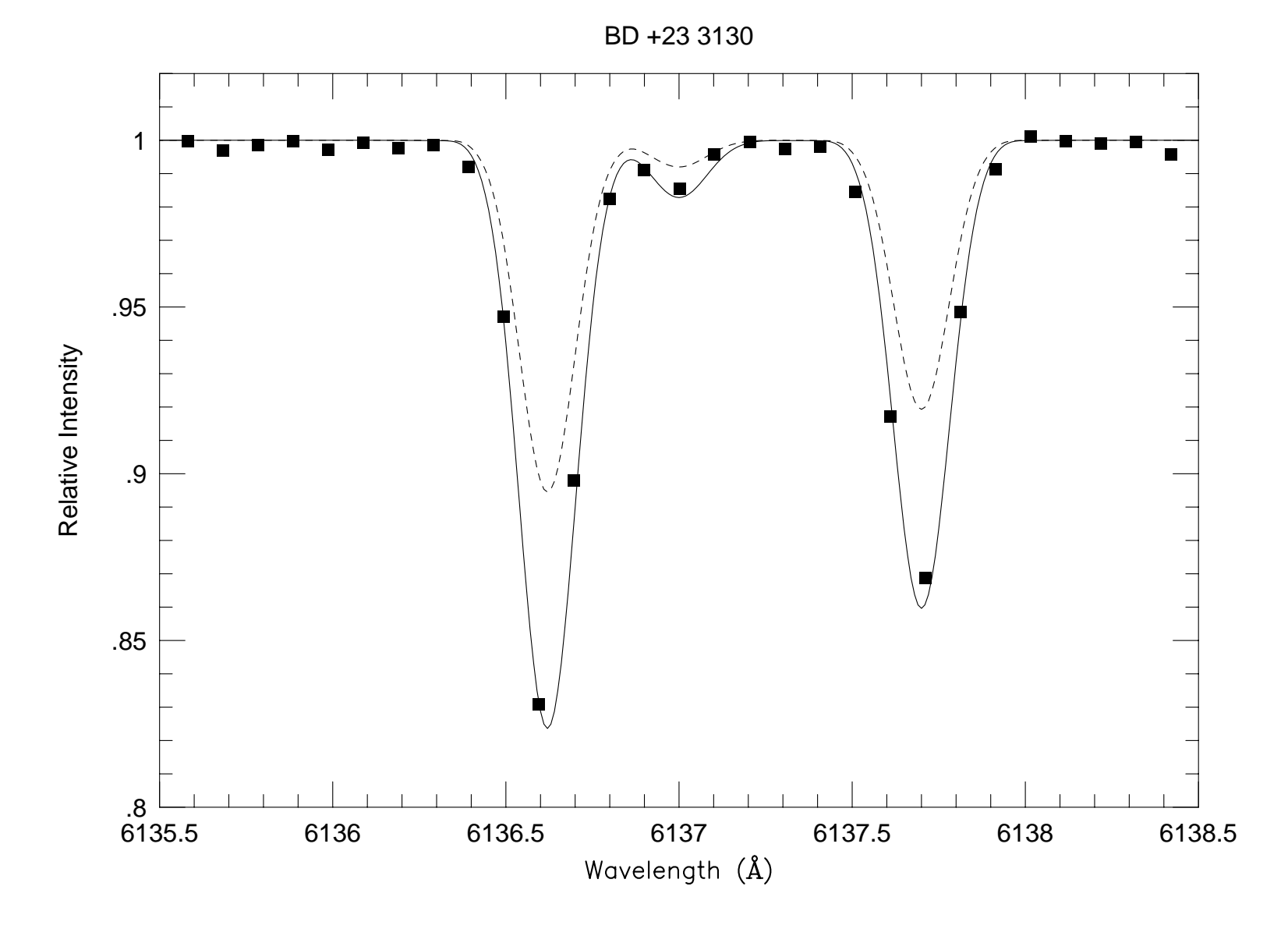


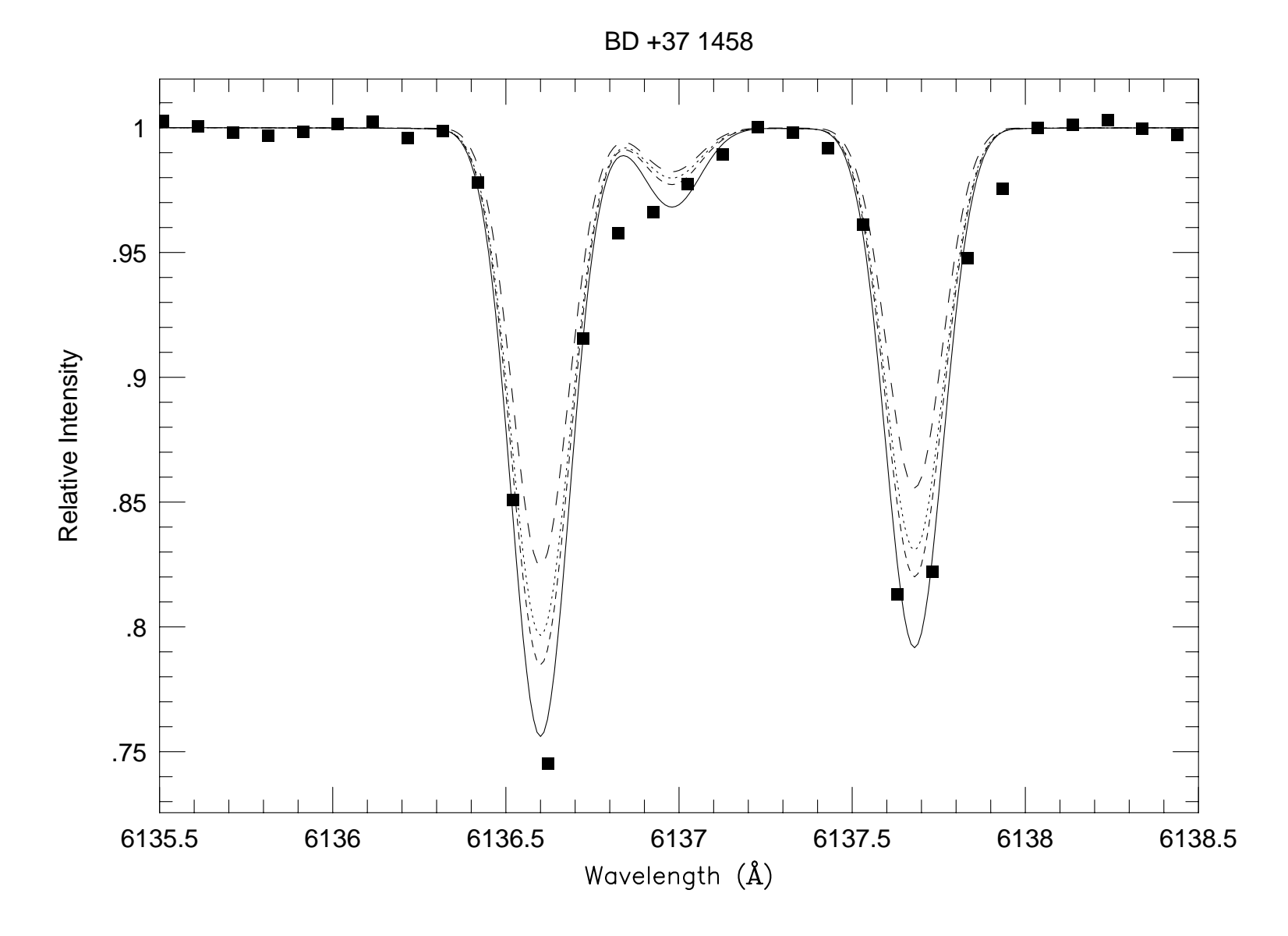




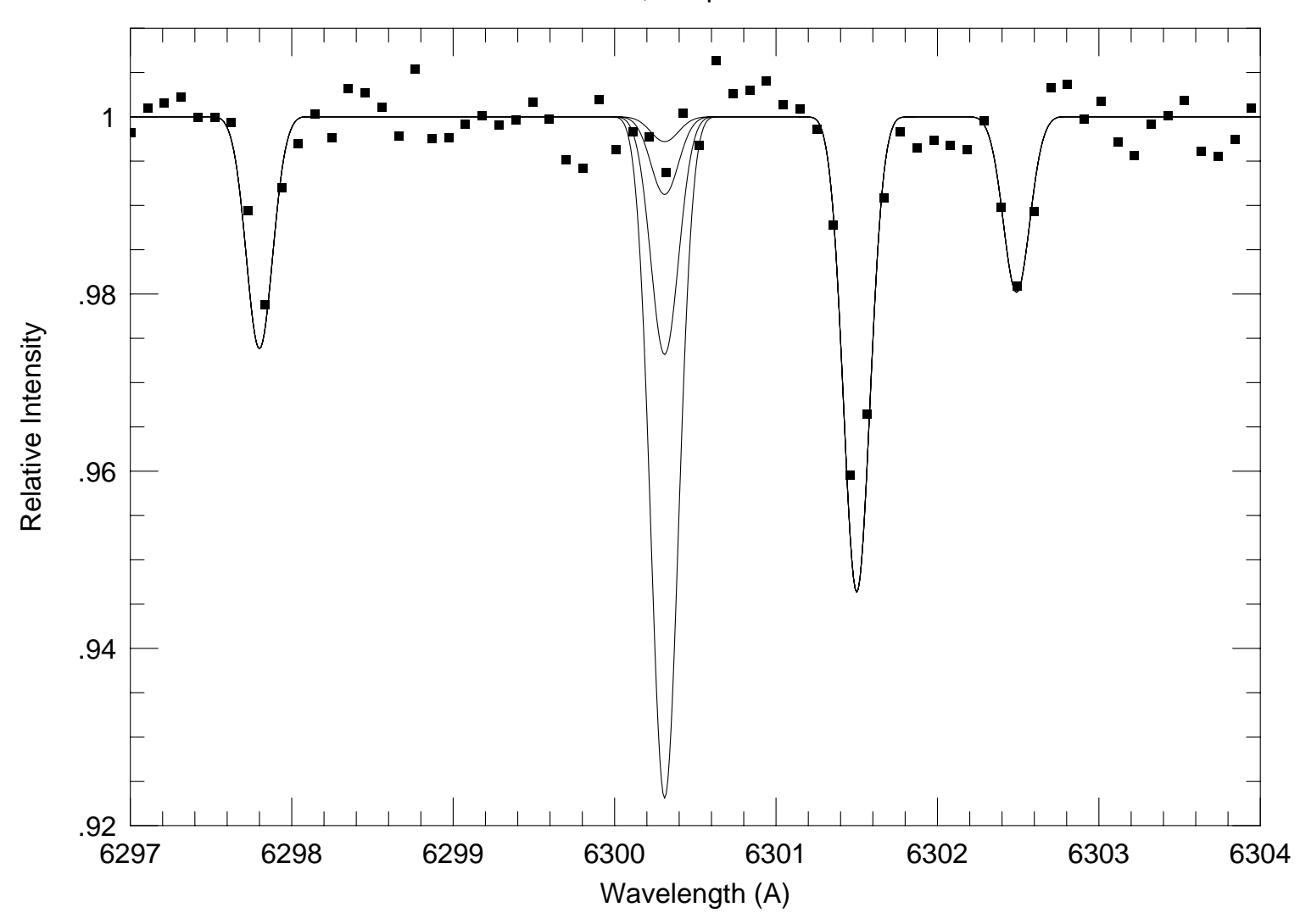




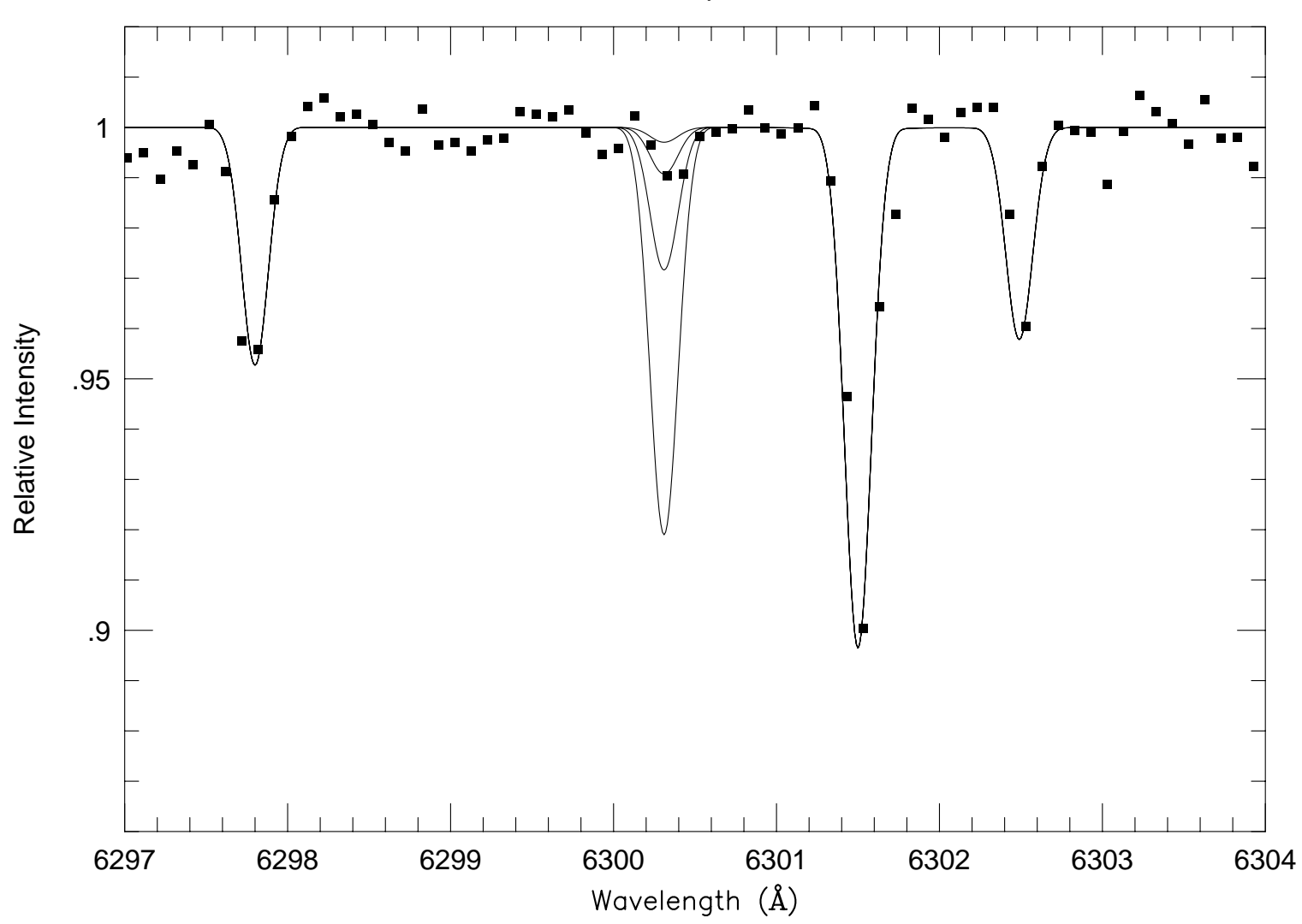




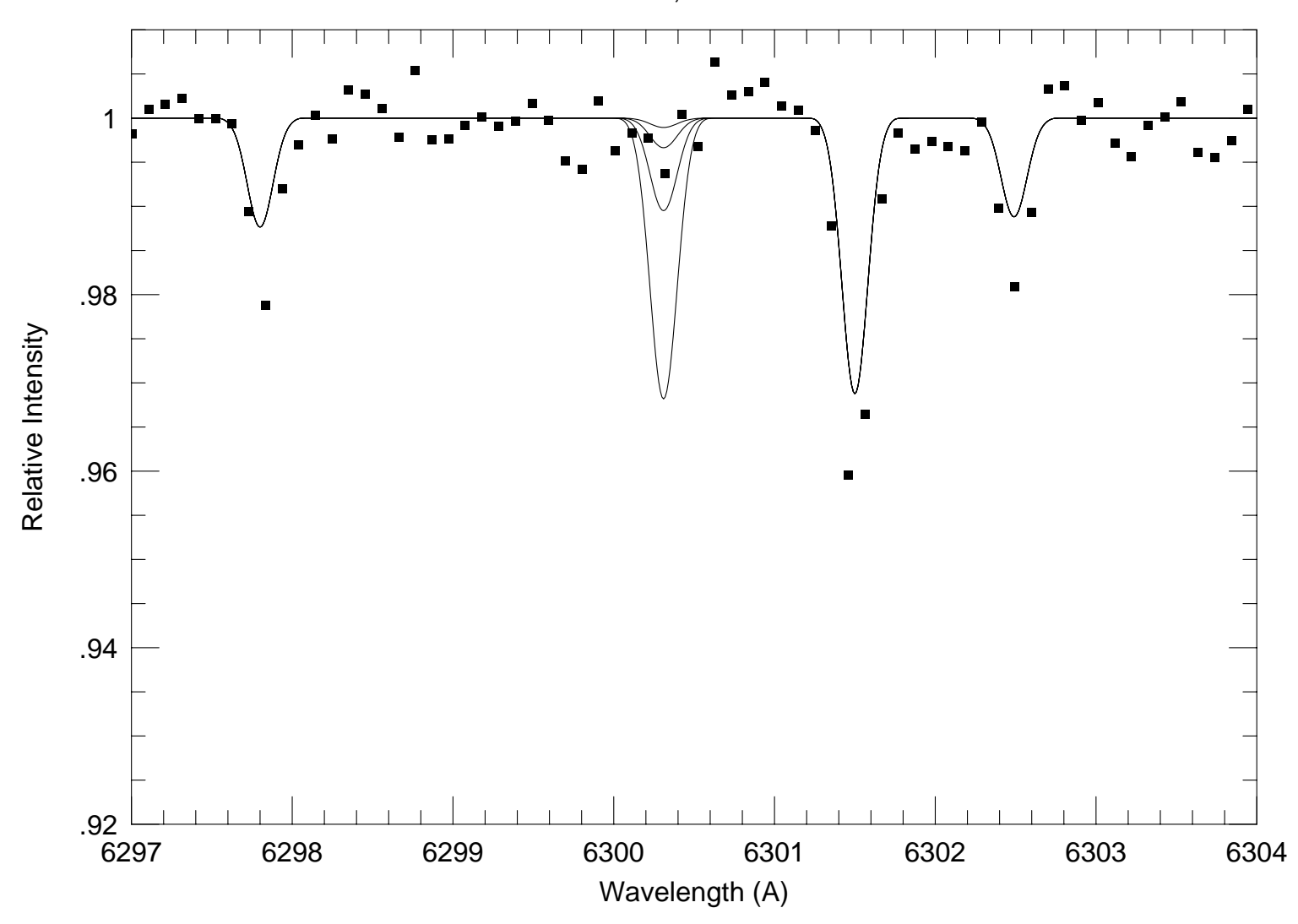
BD +23 3130, Adopted Parameters

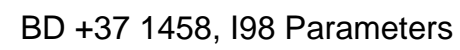


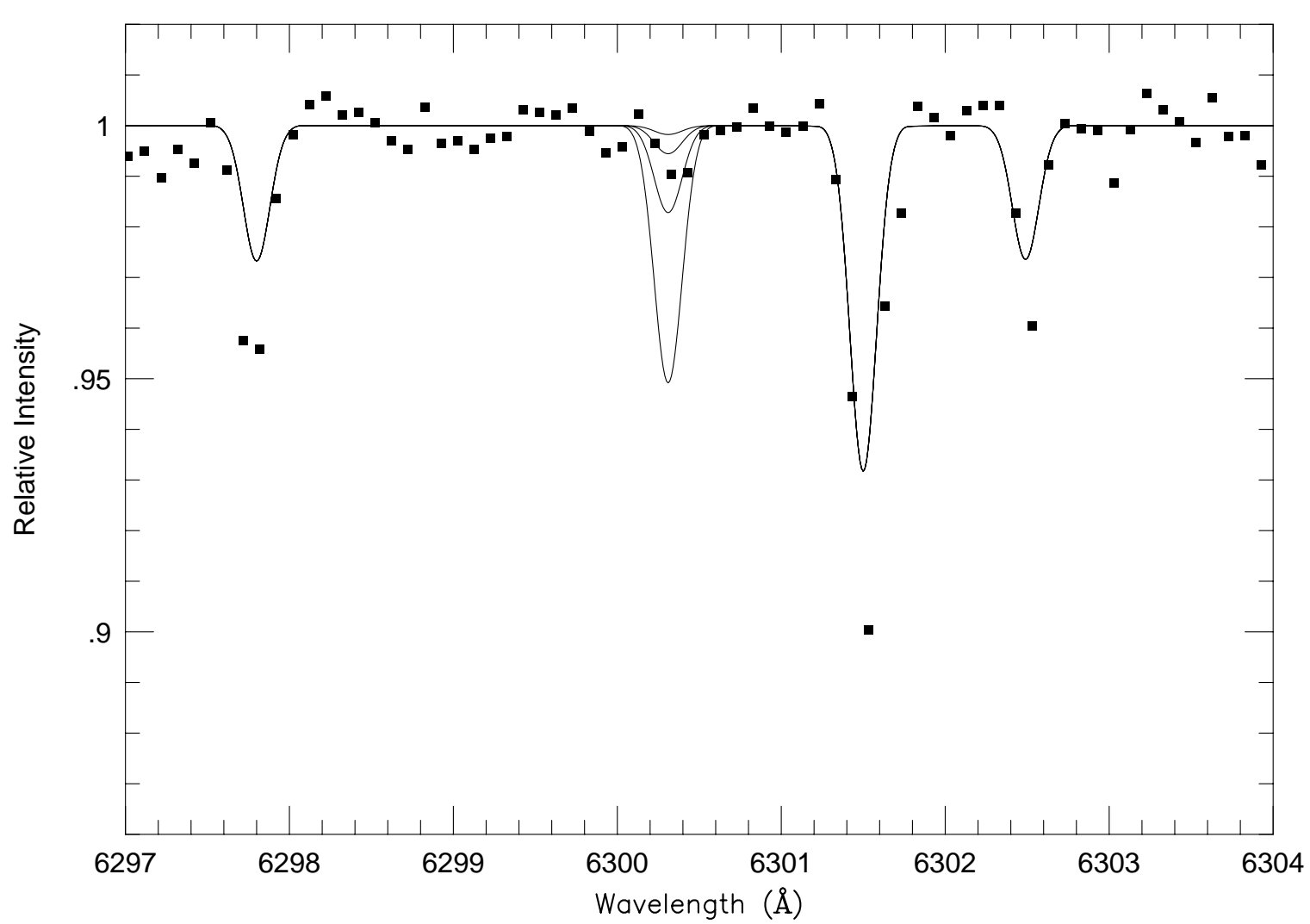




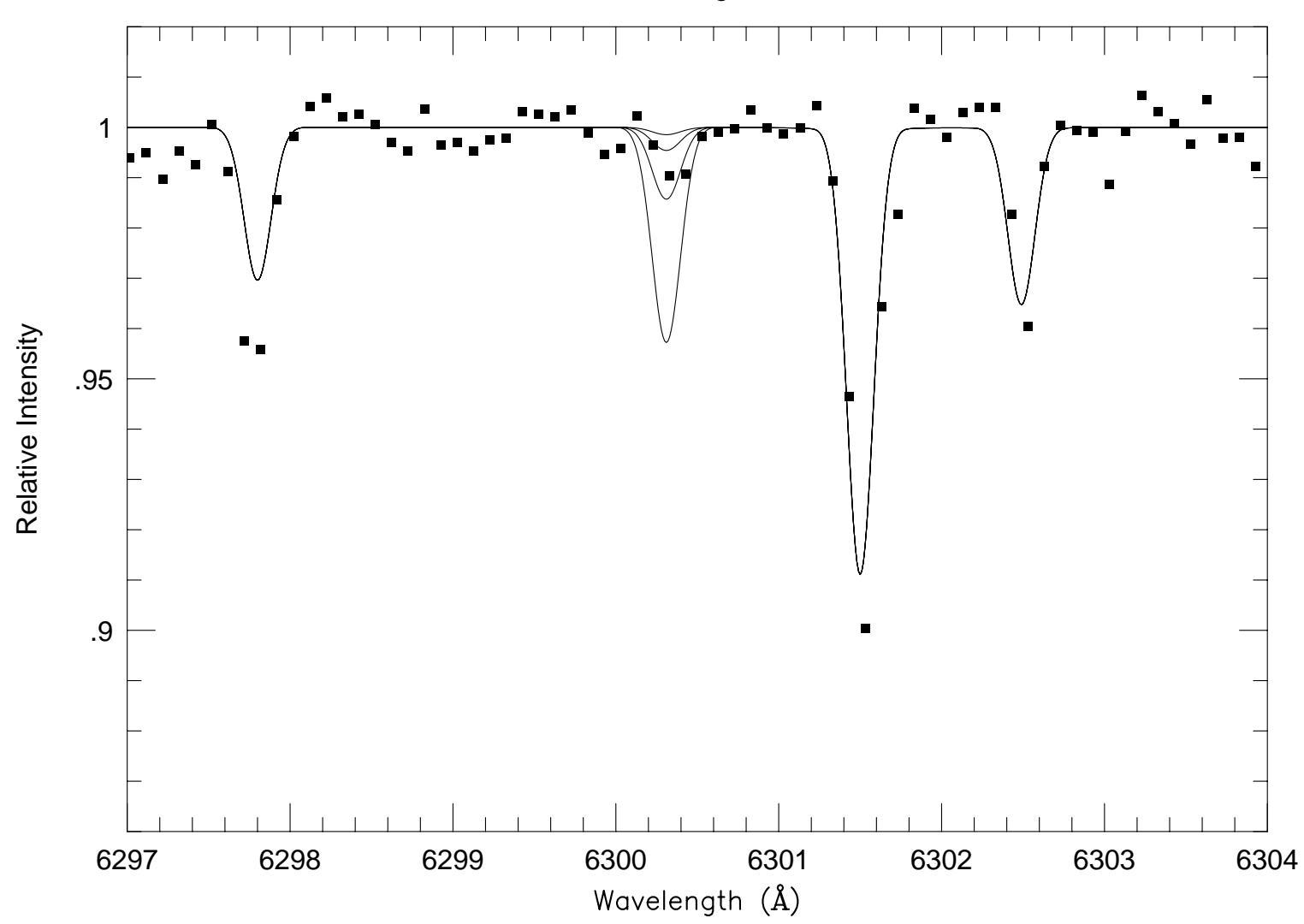
BD +23 3130, I98 Parameters



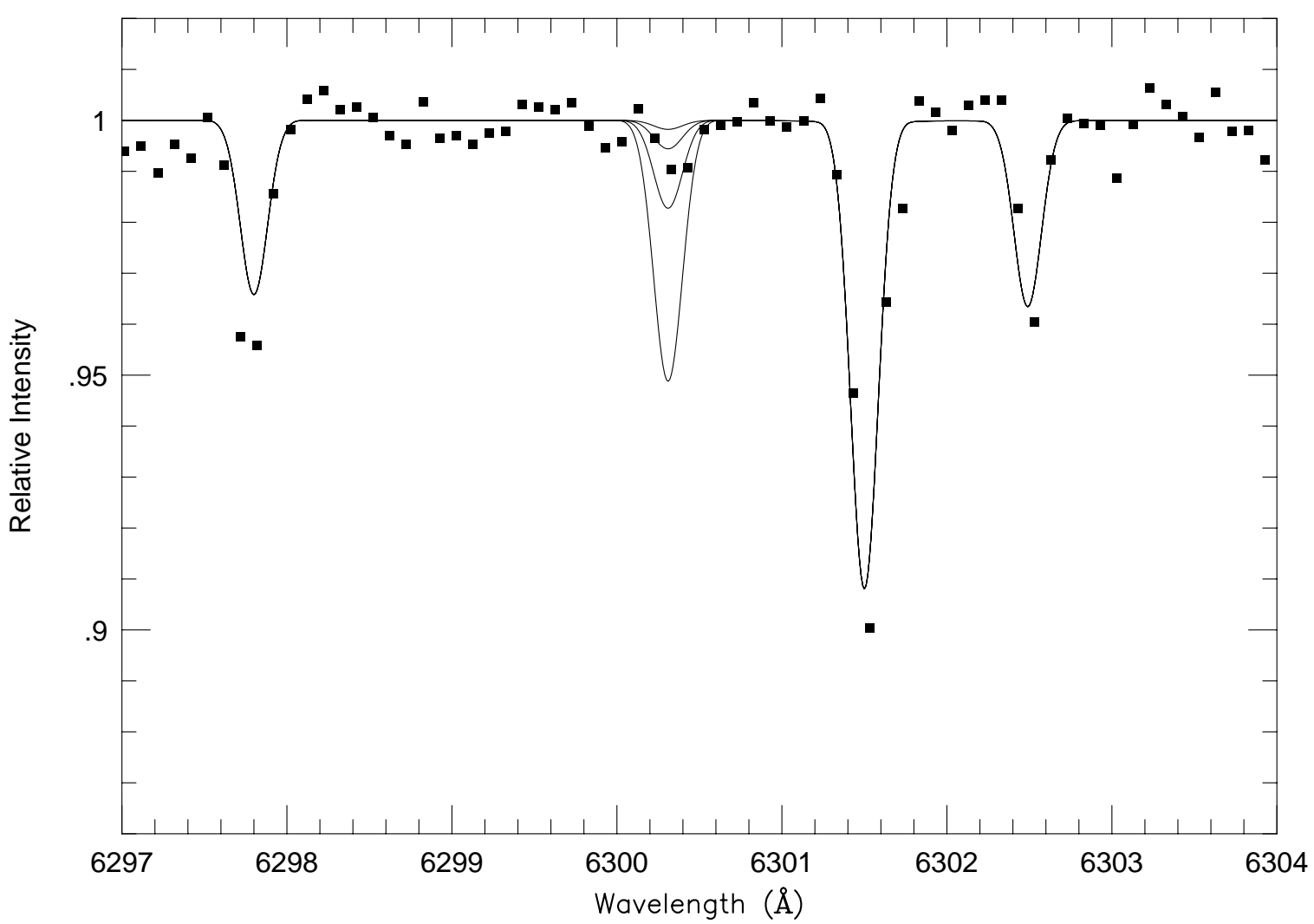




BD+37 1458, B99-King 1993 Parameters







REFERENCES

Abia, C. & Rebolo, R. 1989, ApJ, 347, 186.

Anders, E. & Grevesse, N. 1989, Geochim. Cosmochim. Acta, 53, 197.

Arnett, D. 1995, ARA&A, 33, 115.

Balachandran, S. & Carney, B. W. 1996, AJ, 111, 946.

Bessell, M. S., Hughes, S. & Cottrell, P. L. 1984, Pub. Astr. Soc. Australia, 5, 547.

Bessell, M. S., Sutherland, R. S. & Ruan, K. 1991, ApJ, 383, 71.

Beveridge, R. C. & Sneden, C. 1994, AJ, 108, 285.

Biemont, E., Baudoux, M., Kurucz, R. L., Ansbacher, W. & Pinnington, E. H. 1991, A&A, 249, 539.

Blackwell, D. E., Ibbetson, P. A., Petford, A. D. & Shallis, M. J. 1979a, MNRAS, 186, 633.

Blackwell, D. E., Petford, A. D. & Shallis, M. J. 1979b, MNRAS, 186, 657.

Blackwell, D. E., Petford, A. D., Shallis, M. J. & Simmons, G. J. 1980, MNRAS, 191, 445.

Blackwell, D. E., Shallis, M. J. & Simmons, G. J. 1982a, MNRAS, 199, 33.

Blackwell, D. E., Petford, A. D., Shallis, M. J. & Simmons, G. J. 1982b, MNRAS, 199, 43.

Blackwell, D. E., Petford, A. D. & Simmons, G. J. 1982c, MNRAS, 201, 593.

Blackwell, D. E., Booth, A. J., Haddock, D. J., Petford, A. D. & Leggett, S. K. 1986, MNRAS, 220, 549.

Boesgaard, A., King, J. R., Deliyannis, C. P. & Vogt, S. S. 1999, AJ, 117, 492.

Briley, M. M., Bell, R. A., Hesser, J. E. & Smith, G. H. 1994, Can. J. Phys., 72, 772.

Carbon, D. F., Langer, G. E., Butler, D., Kraft, R. P., Trefzger, C. F., Suntzeff, N. B., Kemper, E. & Romanishin, W. 1982, ApJS, 49, 207.

Carney, B. W. 1983 AJ, 83 610.

Carney, B. W., Latham, D. W., Laird, J. B. & Aguilar, L. A. 1994, AJ, 107, 2240.

Cavallo, R. M., Pilachowski, C. A. & Rebolo, R. 1997, PASP, 109, 226.

Chaboyer, B., Demarque, P., Kernan, P. J. & Krauss, L. M. 1998, ApJ, 494, 96.

Djorgovski, S. 1993, in ASP Conf. Ser., 50, 373.

Fuhr, J. R., Martin, G. A. & Weise, W. L. 1988, J. Phys. Chem. Ref. Data, 17, Suppl. No. 4, 1.

Fuhrmann, K., Axer, M. & Gehren, T. 1995, A&A, 301, 492.

ESA 1997. The Hipparchos & Tycho Catalogues (ESA SP-1200) (Noordwijk: ESA).

Garz, T. 1973, A&A, 26, 471.

Gonzalez, G. & Wallerstein, G. 1998, AJ(in press).

Hanson, R. B., Sneden, C., Kraft, R. P. & Fulbright, J. P. 1998, AJ, 116, 1286.

Hoffleit, D., 1964, Bright Star Catalog, Yale University Observatory

Israelian, G., Garcia Lopez, R. J. & Rebolo, R. 1998, ApJ, 507, 805.

King, J. R. 1993, AJ, 106, 1206.

Kisselman, D. & Nordlund, A. 1995, A&A, 302, 578.

Kraft, R. P. 1994, PASP, 106, 553.

Kraft, R. P., Sneden, C., Smith, G. H., Shetrone, M. D., Langer, G. E. & Pilachowski, C. A. 1997, AJ, 113, 279.

Kroll, S. & Kock, M. 1987, A&AS, 67, 225.

Kurucz, R. L. 1992, private communication.

Lambert, D. L. 1978, MNRAS, 183, 249.

Lambert, D. L. & Warner, B. 1968, MNRAS, 138, 181.

Martin, G. A., Fuhr, J. R. & Wiese, W. L. 1988, J. Phys. Chem. Ref. Data, 17, Suppl. No. 3, 1.

McWilliam, A. 1997, ARA&A, 35, 503.

McWilliam, A., Preston, G. W., Sneden, C. & Searle, L. 1995, AJ, 109, 2757.

Nissen, P. E., Gustafsson, B., Edvardsson, B. & Gilmore, G. 1994, A&A, 285, 440.

O'Brian, T. R., Wickliffe, H. E., Lawler, J. E., Whaling, W. & Brault, J. W. 1991, J. Opt. Soc. Am. B, 8, 1185.

Rood, R. T. & Crocker, D. A. 1985, in ESO Workshop on Production and Distribution of C, N, O Elements, ed. I. J. Danziger, F. Matteucci, & K. Kjar (ESO, Garching), p. 61.

Schlegel, D. J., Finkbeiner, D. P. & Davis, M. 1998, ApJ, 500, 525.

Schuster, W. J. & Nissen, P. E. 1989, A&A, 222, 69.

Shetrone, M. D. 1996, AJ, 112, 1517.

Smith, G. & Raggett, D. S. J. 1981, J. Phys. B. 14, 4015.

Sneden, C. 1973, ApJ, 184, 839.

Sneden, C., Kraft, R. P., Prosser, C. F. & Langer, G. E. 1991, AJ, 102, 2001.

Sneden, C., Kraft, R. P., Langer, G. E., Prosser, C. F. & Shetrone, M. D. 1994, AJ, 107, 1773.

Sneden, C., Kraft, R. P., Shetrone, M. D., Smith, G. H., Langer, G. E. & Prosser, C. F. 1997, AJ, 114, 1964.

Stetson, P. B. & Harris, W. E. 1988, AJ, 96, 909.

Straniero, O. & Chieffi, A. 1991, ApJS, 76, 525.

Suntzeff, N. B. 1993, in ASP Conf. Ser., 48, 167.

Takeda, Y. 1995, PASJ, 47, 463.

Thevenin, F. 1989, A&AS, 77, 137.

Tomkin, J., Lemke, M., Lambert, D. L. & Sneden, C. 1992, AJ, 104, 1568.

VandenBerg, D. A. 1985, in ESO Workshop on Production and Distribution of C, N, O Elements, ed. I. J. Danziger, F. Matteucci & K. Kjar (ESO, Garching), p. 73.

VandenBerg, D. A. 1992, ApJ, 391, 685.

Vogt, S. S. 1987, PASP, 99, 1214.

Weise, W. L., Smith, M. W. & Miles, B. M. 1969, NBS Ref. Data. Ser.

Weise, W. L. & Martin, G. A. 1980, NSRDS-NBS 68 (U.S. Gov. Printing Office, Washington).

Zinn, R. & West, M. J. 1984, ApJS, 55, 45.

This plano tables was prepared with the AAS LATEX macros v4.0.